5-fluorouracil matrix tablets

6.4.1 Preformulation studies

The following preformulation studies were performed for 5-fluorouracil (5-FU).

Screening studies

The characterization of drugs and polymers were carried out using DSC and FT-IR. DSC thermogram and FT-IR spectra of pure 5-FU is again mentioned in screening studies to avoid inconvenience and for easy comparison.

a. Differential Scanning Calorimetry (DSC): DSC studies were carried out for 5-fluorouracil (5-FU) and its combination with polymers in 1:1 ratio and the thermograms obtained are presented in Figure 86 and 87. From the thermograms it was evident that decomposition temperature of 5-fluorouracil (282 °C) did not change when it was mixed with excipients (282.58 °C). Hence, it may be inferred that there was no interaction between 5-FU and polymers used in the preparation of tablets.

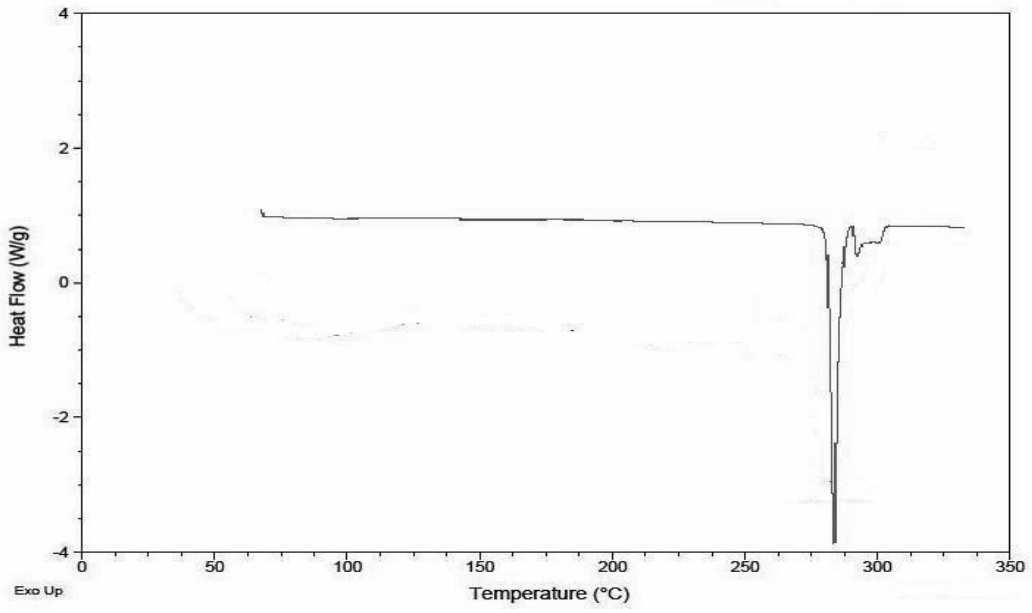

Figure 86: DSC thermogram of 5-fluorouracil (5-FU)

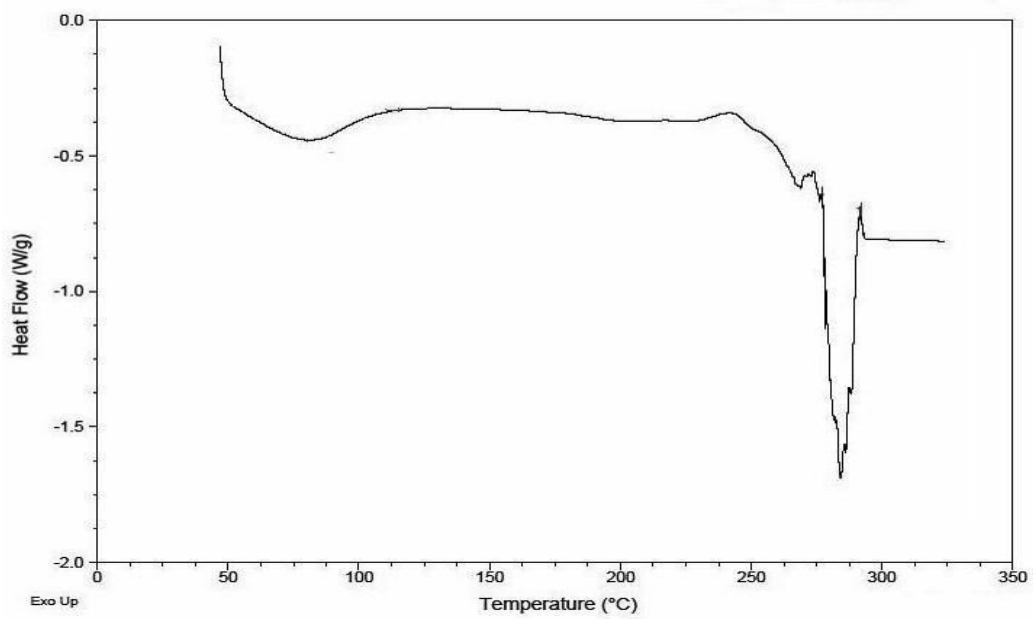

Figure 87: DSC thermogram of 5-fluorouracil (5-FU) with excipients

b. Fourier transform infrared spectroscopy: The compatibility between the drug and polymer was compared by FT-IR spectra. The position of peak in FT-IR spectra of pure 5-fluorouracil is compared with those in FT-IR spectra of 5-fluorouracil plus excipients. It was observed that, there was no disappearance or shift in band position of functional groups in spectrum of 5-fluorouracil alone and with excipients, which proved that 5-fluorouracil and excipients were compatible. Hence, it can be concluded that drug can be used with selected polymer without causing instability in the formulation. The spectra are reported in Figures 88 and 89. The data is summarized in table 42.

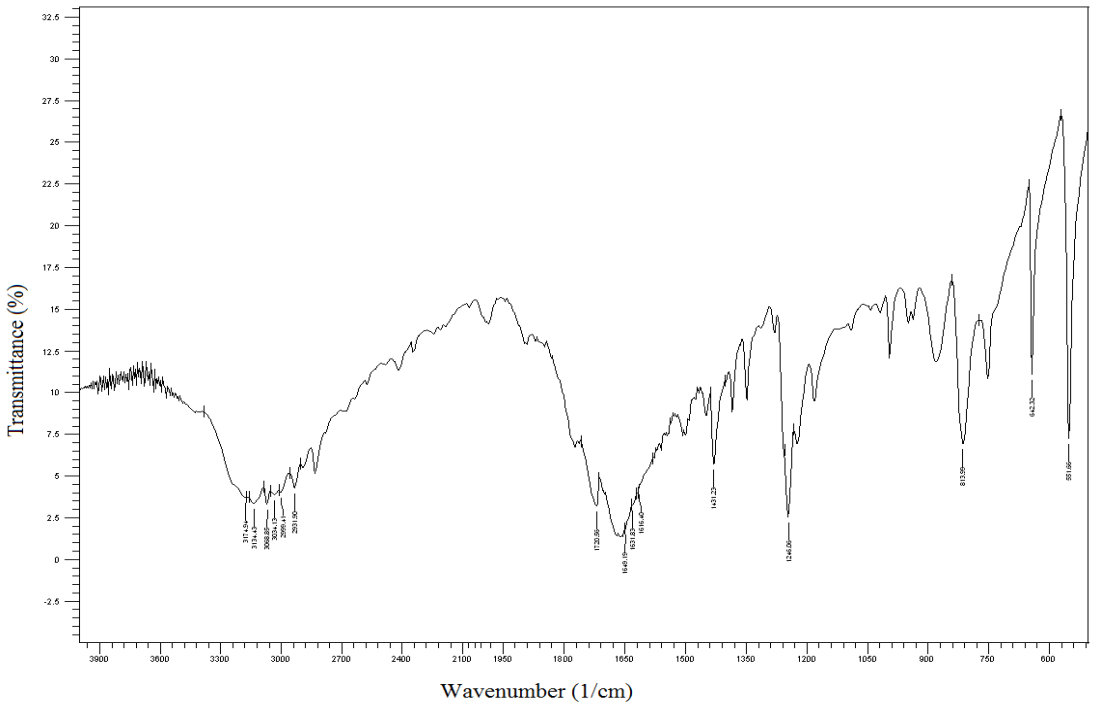

Figure 88: FT-IR Spectra of pure 5-fluorouracil (5-FU)

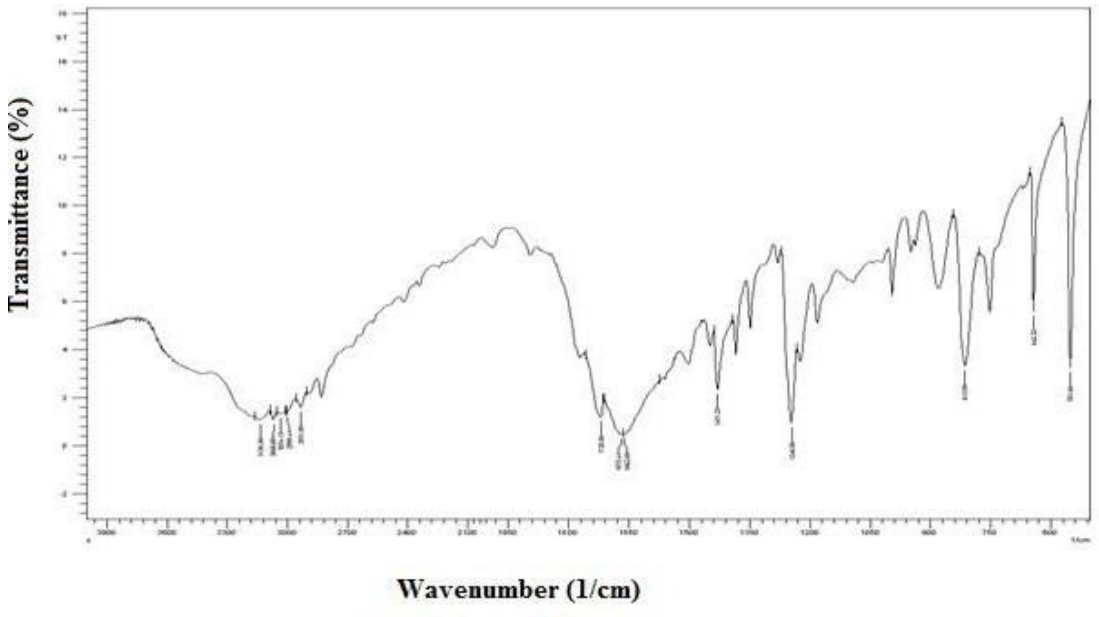

Figure 89: FT- IR Spectra of 5-fluorouracil (5-FU) with excipients

Table 42: FT-IR spectra data of 5-fluorouracil (5-FU) and the formulation

Group	Wavenumber (cm^{-1})	
	Drug	**Formulation**
N-H(Stretching) Free	3173.01	3173.21
C=O(Stretch)	1720.58	1720.32
C-N(stretch)	1649.19	1652.21
C-H (in plane)	1243.03	1246.08
C-O	1180.11	1177.11

6.4.2 Viscosity measurement of chitosan-sodium alginate IPEC ratios

IPECs are usually formed by mixing two polymer solutions carrying opposite charges, depending on the pH value of the media the ionic strength and temperature. The pKa value of chitosan is about 6.3 [225] and the pKa of mannuronic acid and guluronic acid of alginate are 3.38 and 3.65 [226] respectively. In 1 % acetic acid solution (pH value was about 4.8), chitosan dissolved with sufficient number of amine group protonated. When mixing with sodium alginate solution, most of the carboxylic groups (about 97 %) on the alginate were expected to be present in the form of COO^- under this condition. The coulombic forces between the amine and carboxylic groups of alginate as well as

hydrophobic interactions will promote the formation of a strongly associated complex. The 4:4 ratio of chitosan to sodium alginate exhibited more interaction and hence showed less viscosity as shown in figure 90.

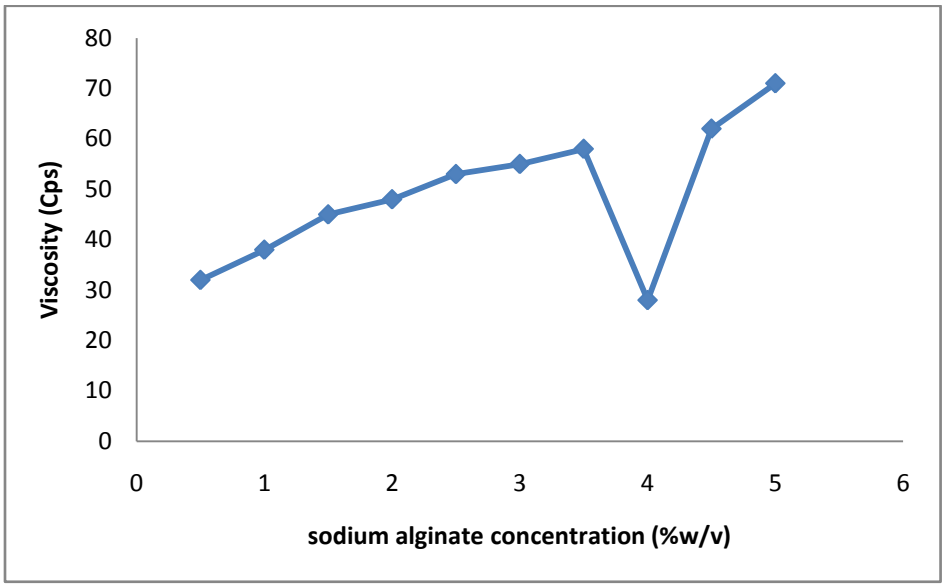

Figure 90: Viscosity measurement of the supernatant solutions of different ratios of chitosan and sodium alginate

6.4.3 Characterization of the chitosan-sodium alginate IPEC

6.4.3.1 Fourier transform infrared spectroscopy (FT-IR)

The chitosan spectrum also exhibited the distinctive absorption bands at 1656 cm^{-1} (C=O stretching in amide group, amide I vibration), 1575 cm^{-1} (–NH_2 bending in non-acetylated 2-aminoglucose primary amine) and 1560 cm^{-1} (N–H bending in amide group, amide II vibration). Absorption bands at 1153 cm^{-1} (antisymmetric stretching of the C–O–C bridge), 1083 and 1031 cm^{-1} (skeletal vibrations involving the C–O stretching) are characteristic of chitosan saccharide structure [227-229]. The FT-IR spectra of chitosan in 2000-1000 cm^{-1} and 1800-1400 cm^{-1} are given in figure 27 and 28 respectively.

In the FT-IR spectrum of sodium alginate two strong absorption peaks at 1611 and 1415 cm^{-1} were observed. They can be assigned to the antisymmetric and symmetric stretching vibration of the carboxylate group, respectively [230]. In addition, the bands around 1320 cm^{-1} (C–O stretching),1130 cm^{-1} (C–C stretching), 1090 cm^{-1} (C–O stretching), 1020 cm^{-1} (C–O–C stretching), and 950 cm^{-1} (C–O stretching) are attributed to its saccharide structure [231]. The FT-IR spectra of sodium alginate in 2000-1000 cm^{-1} and 1800-1400 cm^{-1} are given in figure 91 and 92 respectively.

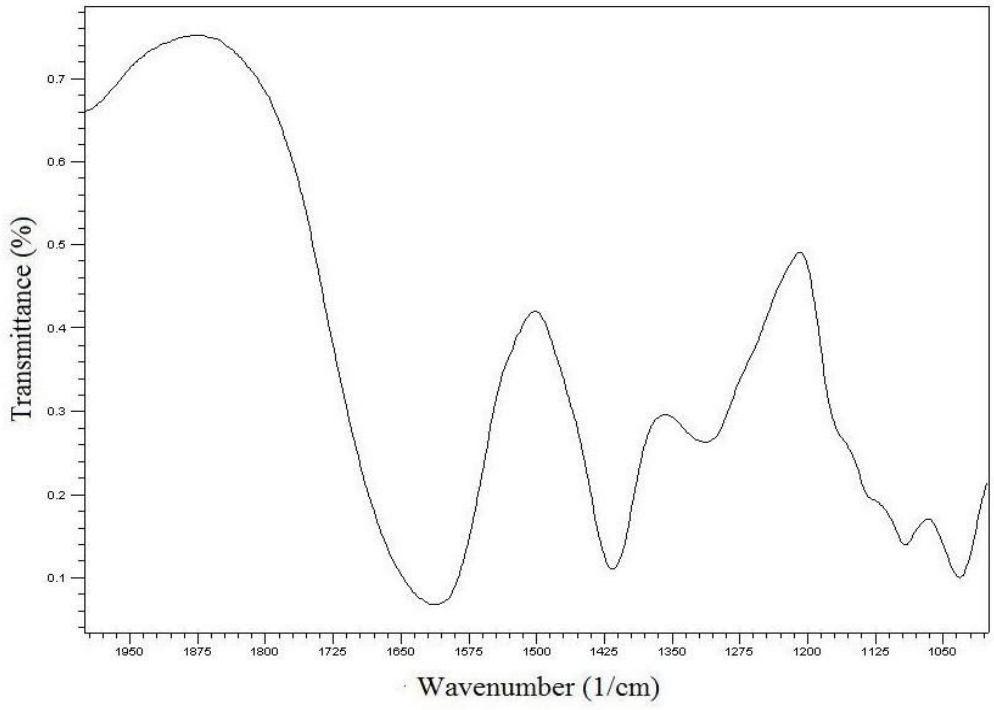

Figure 91: FT-IR spectra of sodium alginate in 2000-1000 cm^{-1}

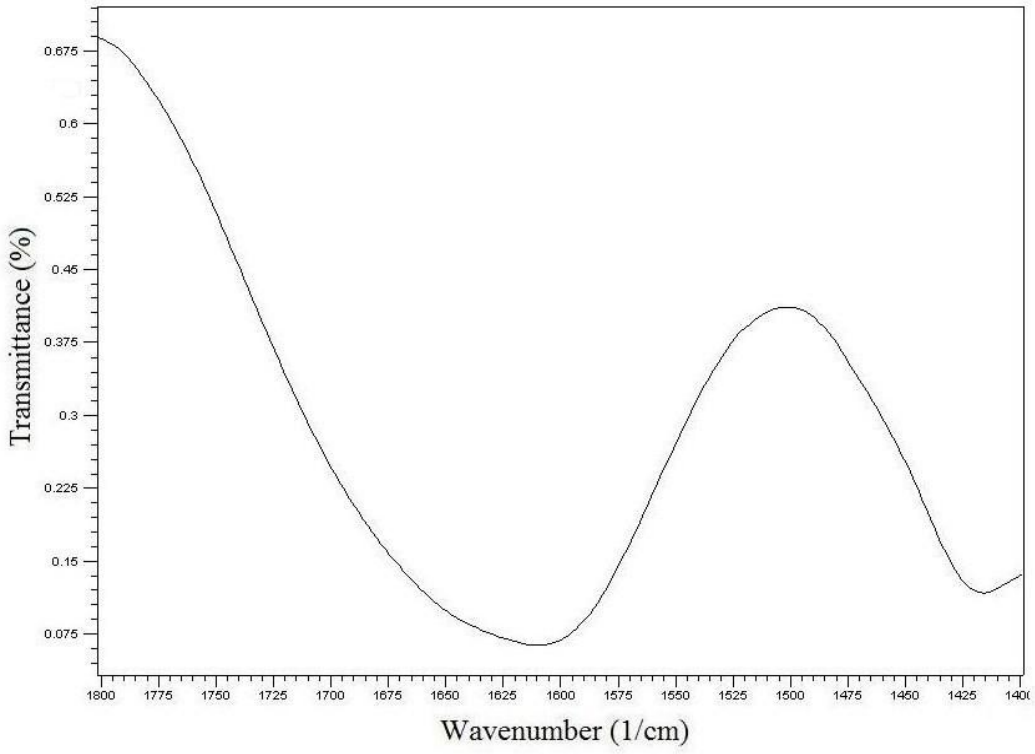

Figure 92: FT-IR spectra of sodium alginate in 1800-1400 cm^{-1}

After complexation, IPEC showed similar spectra to that of sodium alginate but there was shift in position of bands. Band at 1610 and 1415 cm^{-1} in sodium alginate shifted to 1615 and 1419 cm^{-1} in IPEC. The intensity of 1419 cm^{-1} band in IPEC was also reduced indicating that most of the alginate in the IPEC was deprotonated. The shoulder band may be assigned to amide group of chitosan and the broadness of the band ranging 1750–1500 cm^{-1} arised from overlapping bands from amide of chitosan and carboxyl anions of alginate [232,233]. Thus, the above mentioned changes observed in the FT-IR spectra of chitosan after reaction with sodium alginate seems to indicate the formation of IPEC complexes with ionic bonds between carboxylate group of alginate and ammonium group of chitosan. The FT-IR spectra of chitosan-sodium alginate IPEC in 2000-1000 cm^{-1} and 1800-1400 cm^{-1} are given in figure 93 and 94 respectively.

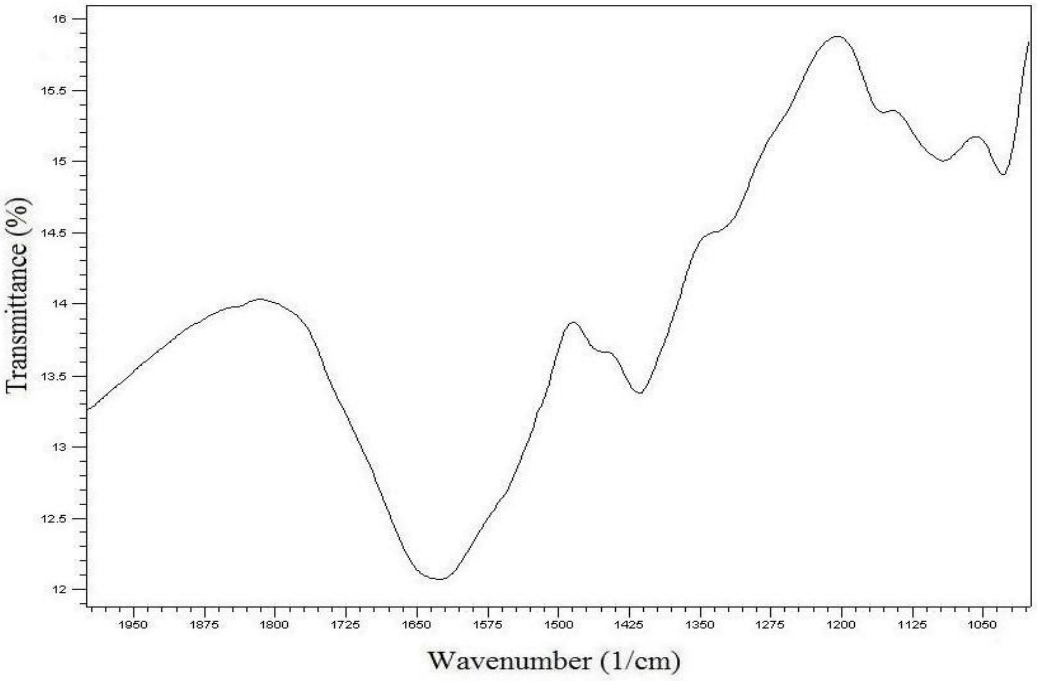

Figure 93: FT-IR spectra of chitosan-sodium alginate IPEC in 2000-1000 cm^{-1}

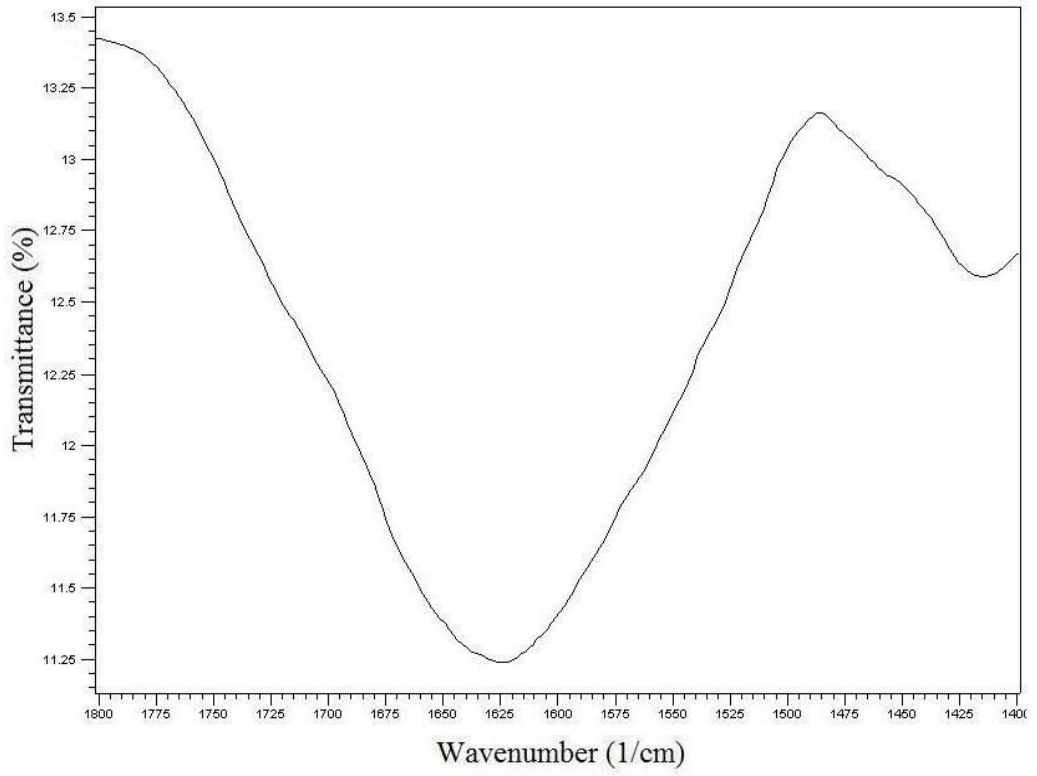

Figure 94: FT-IR spectra of chitosan-sodium alginate IPEC in 1800-1400 cm^{-1}

6.4.3.2 Differential scanning calorimetry (DSC)

It can be seen that thermal degradation of chitosan, sodium alginate and their physical mixture consists of two/three stages but thermal degradation of chitosan/sodium alginate IPEC is more complex. Thermogram of physical mixture is different from that of interpolyelectrolyte complex. It appears to be combination of data obtained for pure polymers. Moreover, it can be seen that the peaks of the IPEC are shifted from those of physical mixture.

As it is known, polysaccharides have a strong affinity for water and their hydration properties depend on their primary and supramolecular structures [234-236]. Moreover, they release water at different temperatures, depending on the different interactions of water with polysaccharide chains. For example, three different kinds of interaction of water and polymer were identified in alginate hydrogels [237,238]. The first one is free water that is released in the region 40–60 °C, the second one is water linked through hydrogen bonds that is released in the region 80–120 °C and finally water more tightly linked through polar interactions with carboxylate groups that is released up to 160 °C. In our study on the DSC thermograms of chitosan, sodium alginate, chitosan/sodium alginate mixtures and only chitosan-sodium alginate complexes, very small peaks (practically not evident on figures) with maximum at around 100–120 °C were observed. The peaks can be related to the water tightly bound to the functional groups of polymers that has not been removed on drying. The second and third stage of polymer degradation corresponds to the thermal decomposition of pure polyelectrolytes or polyelectrolyte complexes and vaporization and elimination of volatile products.

For pure chitosan the second stage started at 240 °C and reached a maximum at 320 °C. According to literature data pyrolysis of chitosan starts by a random split of the glycosidic bonds, followed by a further decomposition to acetic, butyric and lower fatty acids. The DSC thermogram of chitosan is given in figure 33.

For sodium alginate, second stage starts at 190 °C and reaches maximum at 218 °C and a second one at 240 °C. Sodium alginate decomposes by dehydration and degradation to Na_2CO_3 [239]. The DSC thermogram of sodium alginate is shown in figure 95.

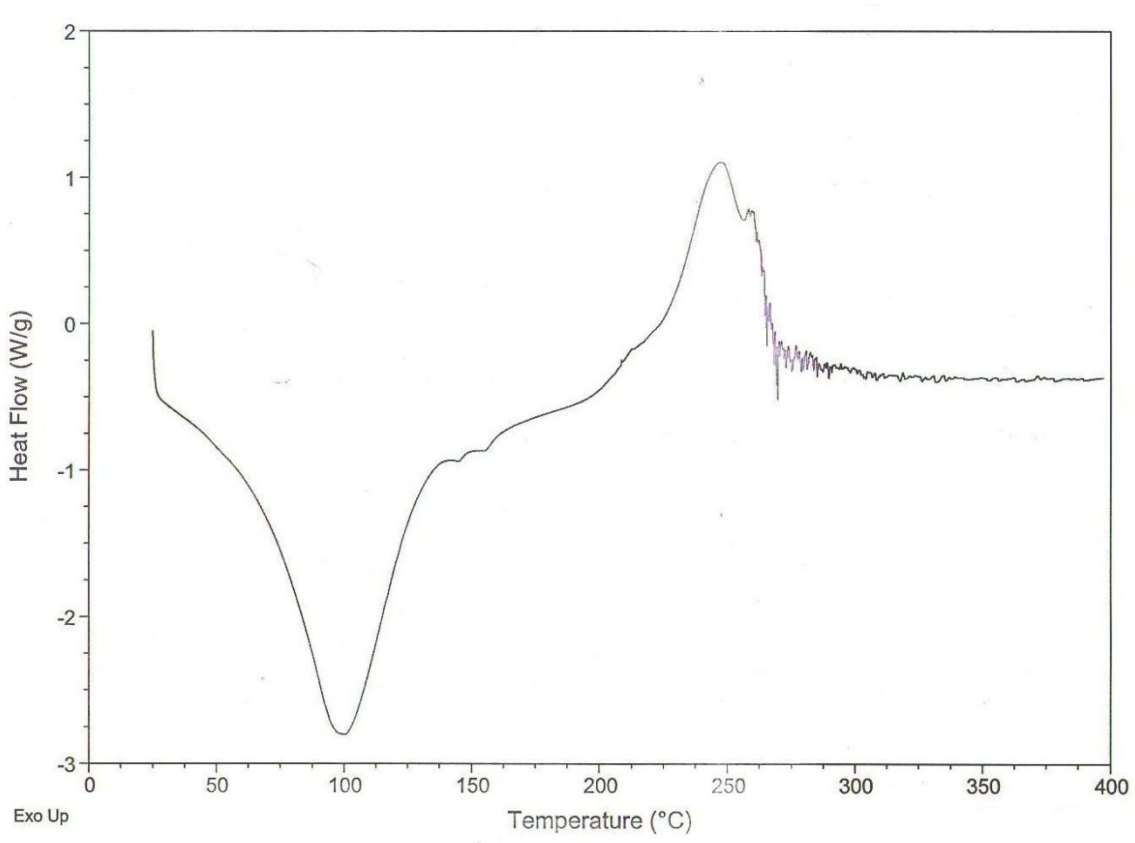

Figure 95: DSC thermogram of sodium alginate

Thermogram of alginate/chitosan physical mixture showed a broader endothermic peak at ~100 °C, which probably represented the coalescence of both isolated endothermic polymer peaks and exothermic peaks at 245 and ~300 °C resulting from individual contribution of alginate and chitosan, respectively. The DSC thermogram of alginate-chitosan physical mixture is given in figure 96.

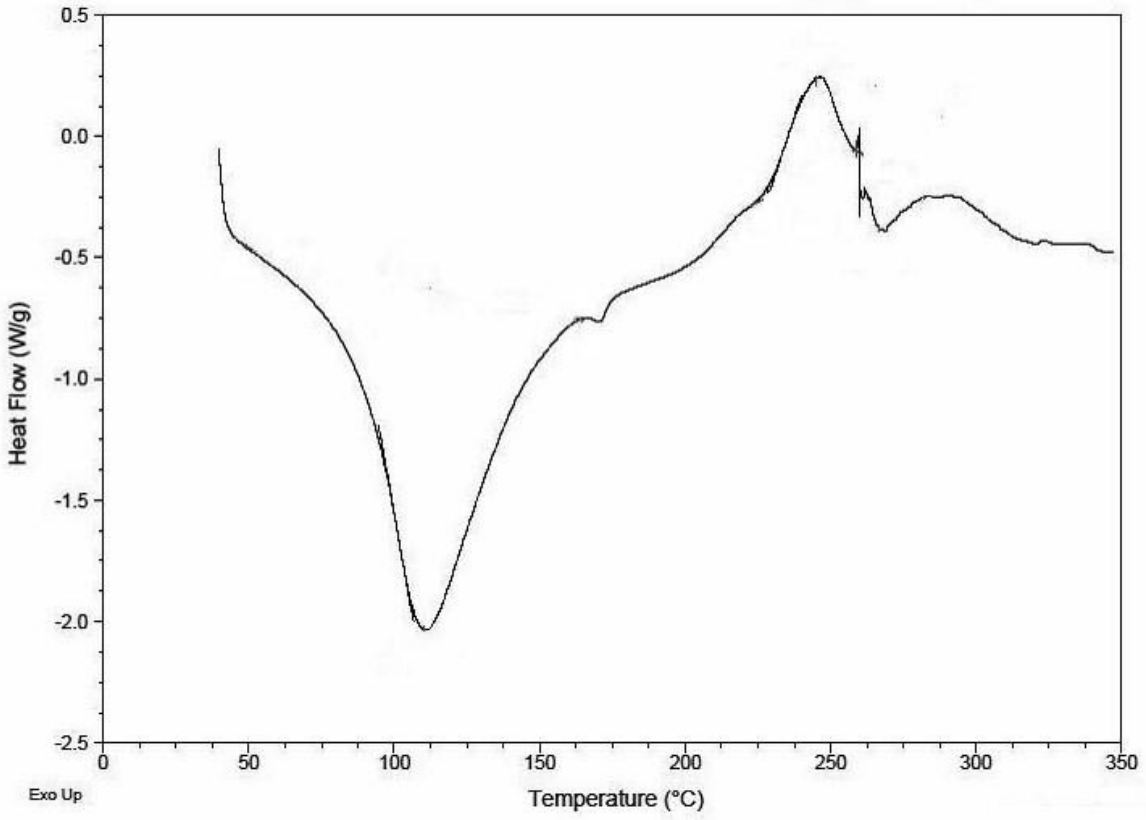

Figure 96: DSC thermogram of chitosan-sodium alginate physical mixture

It could be seen that the peaks of the complexes were shifted from those of physical mixture. Peaks of physical mixture appeared to be combinations of each material but different from those of IPEC probably because complexation of polyelectrolyte's resulted in new chemical bonds. Exothermic peak of IPEC was registered at 289 °C, an intermediate and broader peak value compared to isolate polyelectrolyte's, which was

interpreted as an interaction between both components. This observation indicated that degradation of the IPEC membrane occurred at different temperatures compared to the mixture. Similar results were obtained earlier for chitosan/pectin [240] and chitosan/carboxymethylcellulose complexes [241]. The DSC thermogram of alginate-chitosan IPEC is given in figure 97.

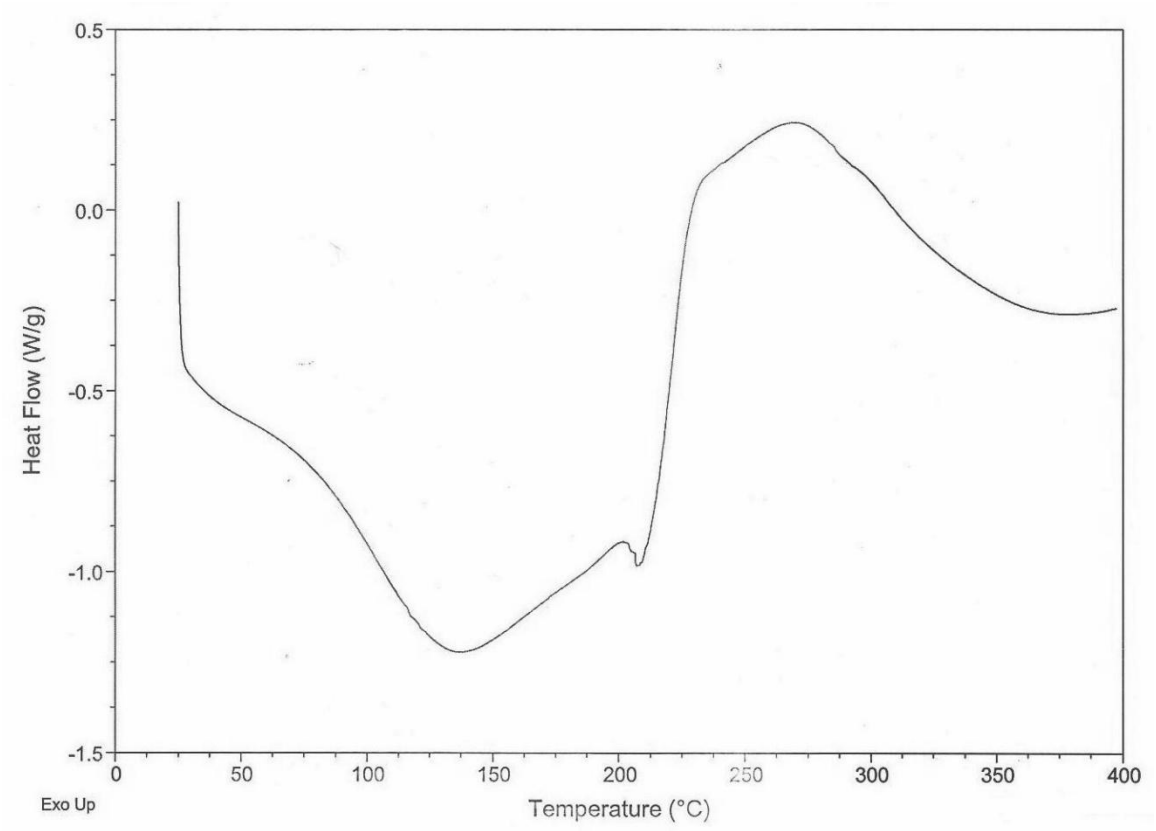

Figure 97: DSC thermogram of chitosan sodium alginate IPEC

6.4.3.3 X-ray diffraction (XRD)

The X-ray diffraction pattern of chitosan is presented in figure 36. The X-ray diffraction pattern of chitosan powder showed two prominent diffraction peaks at 11° (2θ) and 20° (2θ). A shoulder peak appears at 22° (2θ) and also a minor peak appeared at 27° (2θ). The two prominent crystalline peaks at 11° (2θ) and 20° (2θ) are typical fingerprints of chitosan which arre related to the hydrated and anhydrous crystals respectively [203]. The x-ray diffraction pattern of sodium alginate is shown in figure 98. The X-ray diffraction pattern of sodium alginate powder showed prominent diffraction peak at 13° and 21° (2θ) [242].

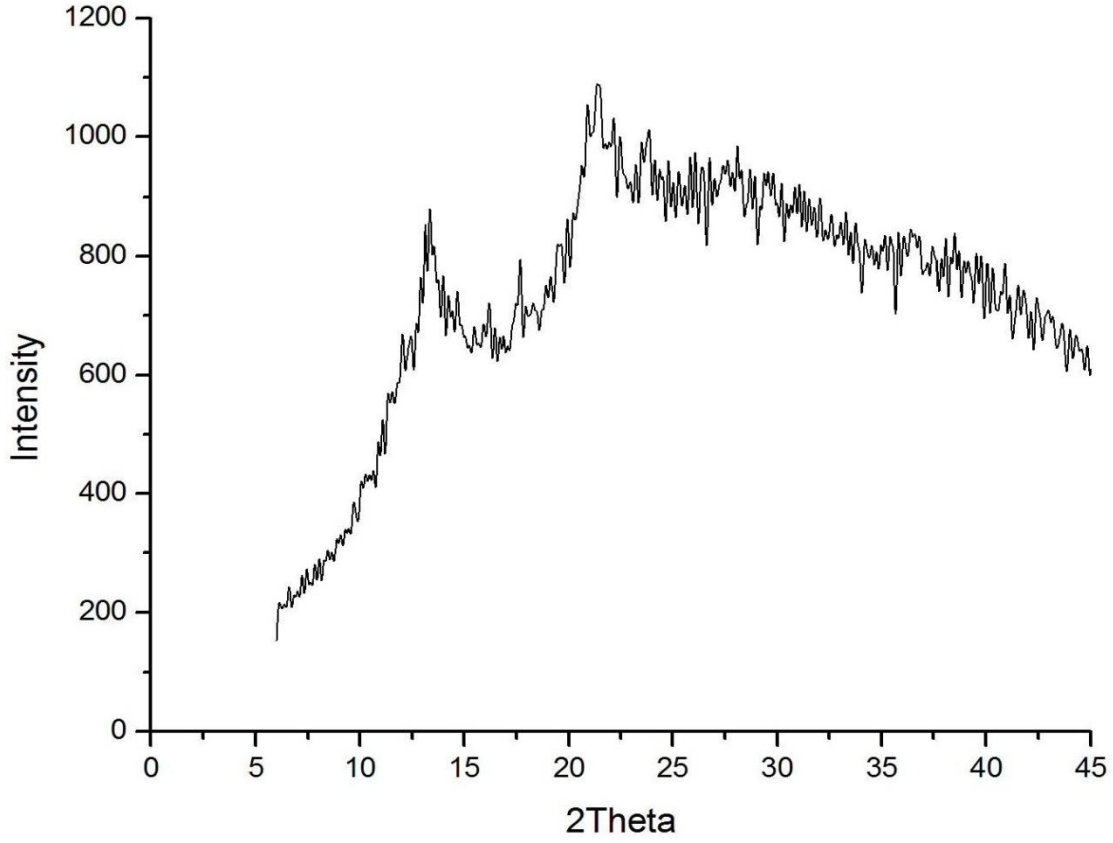

Figure 98: X-ray diffraction spectra of sodium alginate

IPEC X-ray diffraction pattern is given in figure 99. The X-ray diffraction pattern of IPEC powder exhibits prominent and broader diffraction peak at 22° (2θ). Thus, the XRD result revealed that introduction of alginate into chitosan disrupted the crystalline structure of chitosan, which is due to the elimination of hydrogen bonding between amino groups and hydroxyl groups in chitosan [243]. The broad amorphous pattern of the IPEC indicated a good compatibility and strong interaction between alginate and chitosan with a complete dispersion of chitosan chains.

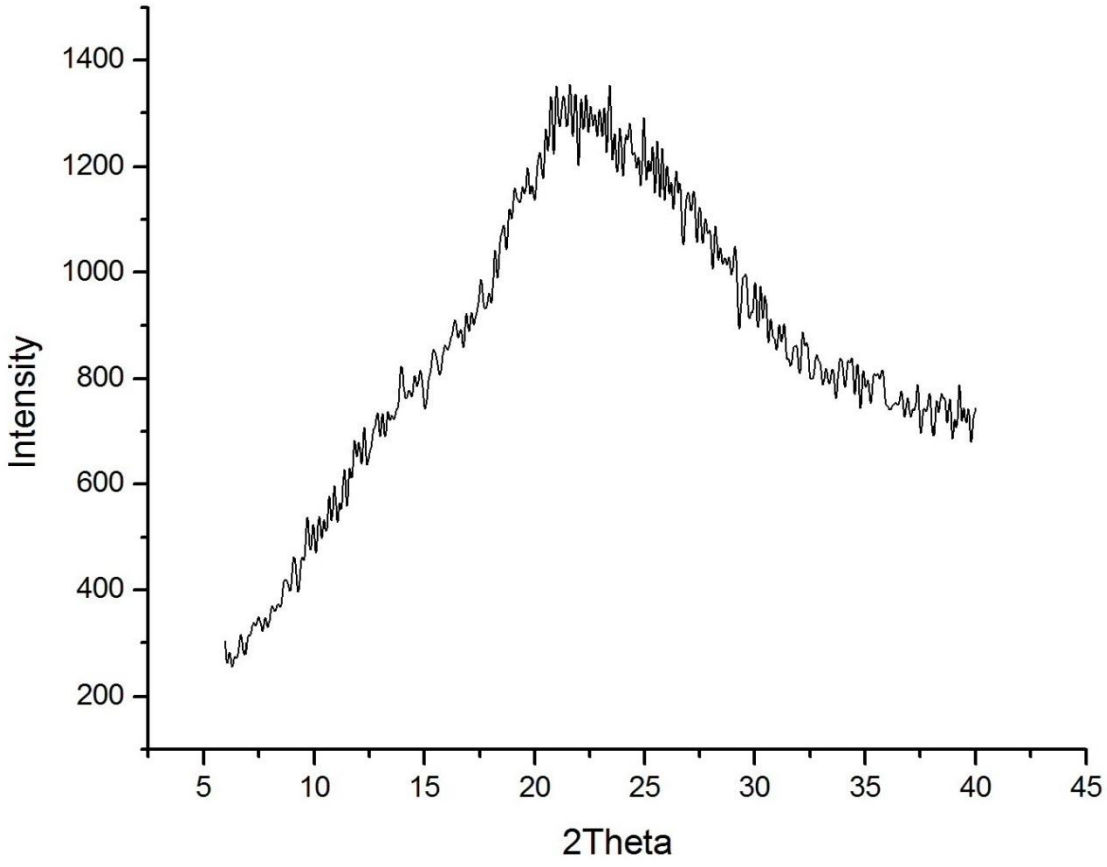

Figure 99: X-ray diffraction spectra of chitosan-sodium alginate IPEC

6.4.4 Evaluation of matrix tablets containing 5-fluorouracil

Tablet properties

The experimental results of tablet evaluation parameters are summarized in table 43. The weights of the prepared tablets were in the range of 149.2-150.2 mg. Tablets of all the batches complied with the weight variation requirement of Indian pharmacopeia and no batch varied more than 10 % of the average weight indicating consistency in the preparation of tablet with minimal batch to batch variation [182]. Thickness of all the tablet formulations ranges from 2.01 to 2.03 mm. Hardness of the tablets ranged from 63 to 72 N. All tablet formulations exhibited friability less than 1 %, indicating compliance with the requirement of USP 29 [183].

Table 43: Evaluation data of 5-FU matrix tablets

Formulation code	Weight (mg)* (n=20)	Thickness (mm)* (n=20)	Hardness (N)* (n=10)	Friability (%) (n=20)	%Drug content* (n=3)
FF1	150.2±0.24	2.01±0.03	65±2	0.21	99.85±0.07
FF2	150.1±0.54	2.01±0.02	72±3	0.09	99.90±0.08
FG1	149.5±0.52	2.03±0.01	66±2	0.18	99.89±0.03
FG2	149.2±0.45	2.01±0.03	63±4	0.19	99.91±0.03
FH1	149.7±0.52	2.01±0.01	70±2	0.08	99.96±0.05
FH2	150.1±0.52	2.03±0.02	71±1	0.08	99.90±0.09
FH3	149.6±1.00	2.02±0.01	72±1	0.09	99.91±0.03
FH4	149.4±0.52	2.01±0.02	71±1	0.10	99.93±0.06
FI1	150.0±1.00	2.02±0.01	71±2	0.09	99.88±0.01
FI2	149.5±0.75	2.01±0.02	70±2	0.08	99.91±0.04
FJ1	150.0±0.53	2.03±0.03	72±2	0.08	99.92±0.03
FJ2	150.1±0.51	2.02±0.02	71±2	0.09	99.89±0.05

***mean± Standard Deviation**

6.4.5 Swelling studies

The swelling behavior of formulations at 37±0.5 °C in phosphate buffer pH 6.8, simulated vaginal fluid pH 4.2 and phosphate buffer pH 7.4 are given in table 44,45,46 and graphically represented in figure 100A, 100B, 101A,101B and 102A, 102B respectively.

The swelling ratios of tablet formulations at various pH environments depend upon the availability of free volume of the expanded polymer matrix, polymer chain relaxation, and ionizable functional groups such as –COOH able to form hydrogen bonds with dissolution medium. The swelling behavior was indicative of the rate at which this formulation absorbed water from dissolution media and swelled. These matrices generally showed a higher ability to swell in neutral medium (phosphate buffer, pH 6.8) than in acidic medium (simulated vaginal pH 4.2) whereas, in phosphate buffer pH 7.4, there was rapid swelling of sodium alginate. The pKa of alginic acid (by virtue of the carboxyl groups on the components of uronic acid residues) ranges between 3.4 and 4.4, depending on the type of alginate and the salts present in the mixture [244]. Therefore, changes in pH from 6.8 to 4.2 influence polymer hydration and alginate gel rheology, due to the immediate conversion of carboxylate anions (sodium alginate) to free carboxyl groups (alginic acid) [245]. The matrices appeared to swell almost from the beginning, a viscous gel mass was created when they came into contact with the phosphate buffer pH 6.8, as observed previously in the other report [246]. In the case of hydration of sodium alginate matrix tablets in acidic medium (simulated vaginal pH 4.2), the outer hydrated surface layer formed around the tablets could be seen to possess a very different consistency to that around sodium alginate tablets which were hydrated in neutral

medium. The hydrated layer (in simulated vaginal pH 4.2) was not viscous and adhesive in nature but represented a tough and rubbery texture; this is probably due to sodium alginate which rapidly converted to alginic acid. The physical mixture of chitosan and sodium alginate formulations exhibited relatively lower swelling index in simulated vaginal pH 4.2 due to gel forming ability of chitosan in acidic pH. In phosphate buffer pH 6.8, also there was higher swelling index as sodium alginate swelled more in neutral pH. This might have lead to weaker electrostatic interaction and lesser attraction of polymer chains leading to more opened structure resulting in higher swelling index. Whereas in case of phosphate buffer pH 7.4, the ability of sodium alginate to form gel around tablet was rapid due to the exposure to basic environment as a result it hinders the chitosan polymer characteristic leading to highest swelling index. IPEC containing tablet formulations exhibited almost similar swelling index for all the buffer solutions. The similarity swelling profiles in both the buffer solutions may be attributed to the lack of availability of free functional group as in physical mixture of polymers or single polymers. However, IPEC containing formulations exhibited relatively lesser swelling index than individual polymers, which is in accordance with the literature reported [247]. The length of 12 nm alginates in an unperturbed state [248] and 5 nm for chitosan [249,250], formed alginate–chitosan IPEC. The formed IEPC did not adapt regular rod-like or toroidal morphologies [251]. Thus there was compact ‘‘scrambled” egg existing in the complexes. Another reason for the decreased swelling index of IPEC might be due to the intra molecular hydrogen bonding between the carboxyl groups of alginate and amine groups of chitosan or hydroxyl group or carboxyl groups may occur elsewhere in the network as suggested earlier [187]. This hydrogen bonding may also result in tightening

of IPEC network leading to a reduced swelling capacity. Further addition of polymers decreased the swelling of FI1 and FI2 formulations containing chitosan and sodium alginate along with IPEC which exhibited gradual swelling index due to the availability of free functional groups of chitosan and sodium alginate polymers. The presence of polymers in lower concentration did not have the ability for chain disentanglement or chain relaxation. Hence gradual swelling appeared for all buffer solutions.

Table 44: Swelling index data of 5-FU formulations FF1-FJ2 in phosphate buffer pH 6.8

Formulation Code	Swelling index Mean ± S.D*							
	Time in Hours							
	1 hour	2 hour	3 hour	4 hour	5 hour	6 hour	7 hour	8 hour
FF1	36 ±0.63	103 ±0.52	198 ±0.26	287 ±0.38	398 ±0.83	532 ±0.58	645 ±0.92	----
FF2	76 ±0.12	135 ±0.93	245 ±0.38	324 ±0.81	478 ±0.11	587 ±0.48	698 ±0.37	----
FG1	42 ±0.82	83 ±0.73	121 ±0.90	152 ±0.28	189 ±0.31	245 ±0.28	314 ±0.52	---
FG2	55 ±0.11	117 ±0.37	178 ±0.82	243 ±0.25	287 ±0.46	312 ±0.76	387 ±0.98	----
FH1	211 ±0.35	261 ±0.73	323 ±0.56	398 ±0.68	469 ±0.73	506 ±0.35	579 ±0.39	623 ±0.75
FH2	219 ±0.82	275 ±0.43	345 ±0.76	412 ±0.67	479 ±0.27	518 ±0.98	591 ±0.35	642 ±0.74
FH3	231 ±0.77	289 ±0.35	367 ±0.62	438 ±0.28	498 ±0.45	536 ±0.82	601 ±0.73	654 ±0.82
FH4	256 ±0.83	326 ±0.28	399 ±0.11	467 ±0.72	562 ±0.72	594 ±0.66	628 ±0.41	687 ±0.37
FI1	260 ±0.52	327 ±0.37	403 ±0.73	473 ±0.55	587 ±0.22	599 ±0.24	642 ±0.82	698 ±0.25
FI2	125 ±0.35	179 ±0.66	211 ±0.45	278 ±0.37	301 ±0.56	358 ±0.23	396 ±0.73	417 ±0.46
FJ1	120 ±0.57	180 ±0.32	215 ±0.36	280 ±0.72	303 ±0.22	351 ±0.12	389 ±0.46	415 ±0.62
FJ2	122 ±0.36	175 ±0.65	210 ±0.47	275 ±0.11	302 ±0.23	352 ±0.74	391 ±0.21	412 ±0.17

***Standard deviation, n = 3**

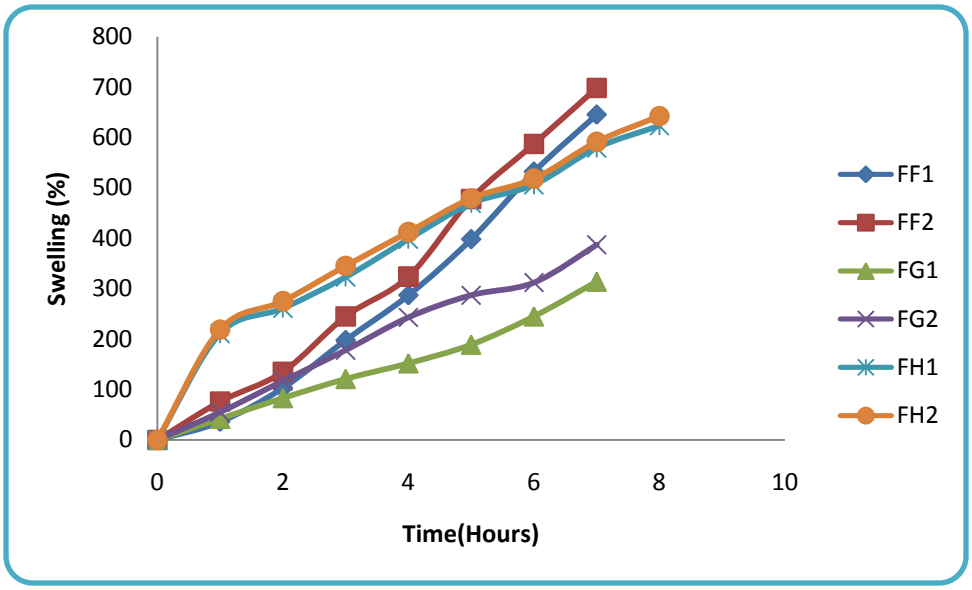

Figure 100A: Swelling index profile for 5-FU formulations FF1-FH2 in phosphate buffer pH 6.8

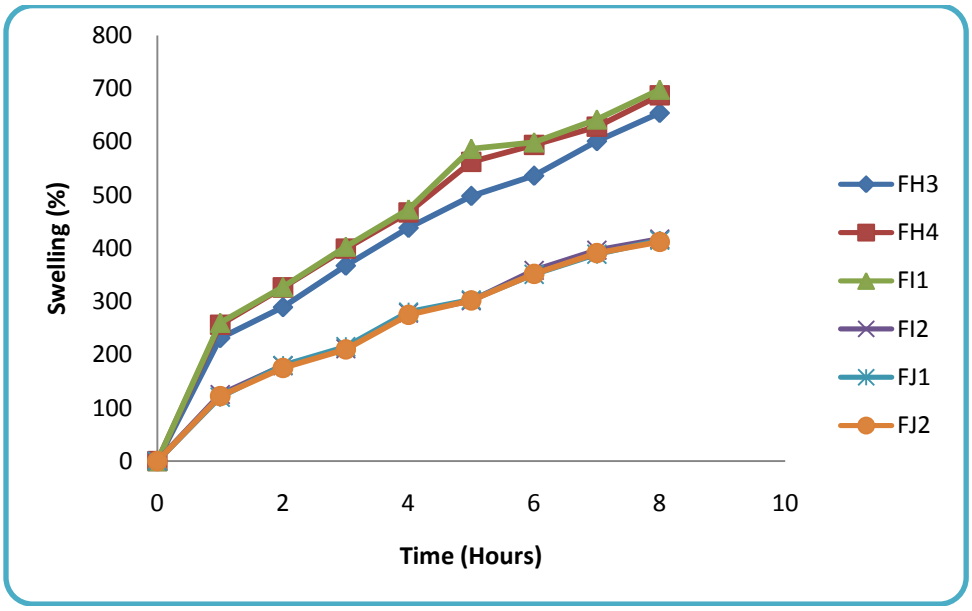

Figure 100B: Swelling index profile for 5-FU formulations FH3-FJ2 in phosphate buffer pH 6.8

Table 45: Swelling index data of 5-FU formulations FF1-FJ2 in SVF pH 4.2

Formulation Code	Swelling index Mean ± S.D*							
	Time in Hours							
	1 hour	2 hour	3 hour	4 hour	5 hour	6 hour	7 hour	8 hour
FF1	35 ±0.95	167 ±0.11	198 ±0.35	235 ±0.25	----	-----	----	----
FF2	54 ±0.66	92 ±0.47	124 ±0.32	196 ±0.36	212 ±0.44	----	-----	-----
FG1	43 ±0.77	79 ±0.36	145 ±0.55	185 ±0.74	----	------	----	----
FG2	68 ±0.22	112 ±0.52	176 ±0.71	231 ±0.35	253 ±0.73	----	----	----
FH1	178 ±0.32	237 ±0.61	326 ±0.53	398 ±0.82	471 ±0.62	502 ±0.35	572 ±0.27	617 ±0.52
FH2	221 ±0.44	279 ±0.39	352 ±0.66	419 ±0.53	482 ±0.82	538 ±0.58	593 ±0.27	632 ±0.92
FH3	245 ±0.66	287 ±0.28	378 ±0.57	442 ±0.42	521 ±0.85	566 ±0.48	603 ±0.55	662 ±0.85
FH4	276 ±0.81	343 ±0.37	401 ±0.54	487 ±0.33	557 ±0.12	589 ±0.46	623 ±0.93	694 ±0.41
FI1	167 ±0.83	198 ±0.28	243 ±0.17	278 ±0.22	323 ±0.92	356 ±0.41	398 ±0.72	410 ±0.37
FI2	189 ±0.46	219 ±0.28	265 ±0.72	305 ±0.15	354 ±0.62	416 ±0.58	443 ±0.29	445 ±0.23
FJ1	192 ±0.37	220 ±0.29	271 ±0.83	309 ±0.58	355 ±0.27	412 ±0.73	445 ±0.35	449 ±0.83
FJ2	190 ±0.38	221 ±0.11	263 ±0.83	310 ±0.72	350 ±0.28	410 ±0.33	439 ±0.37	442 ±0.92

***Standard deviation, n = 3**

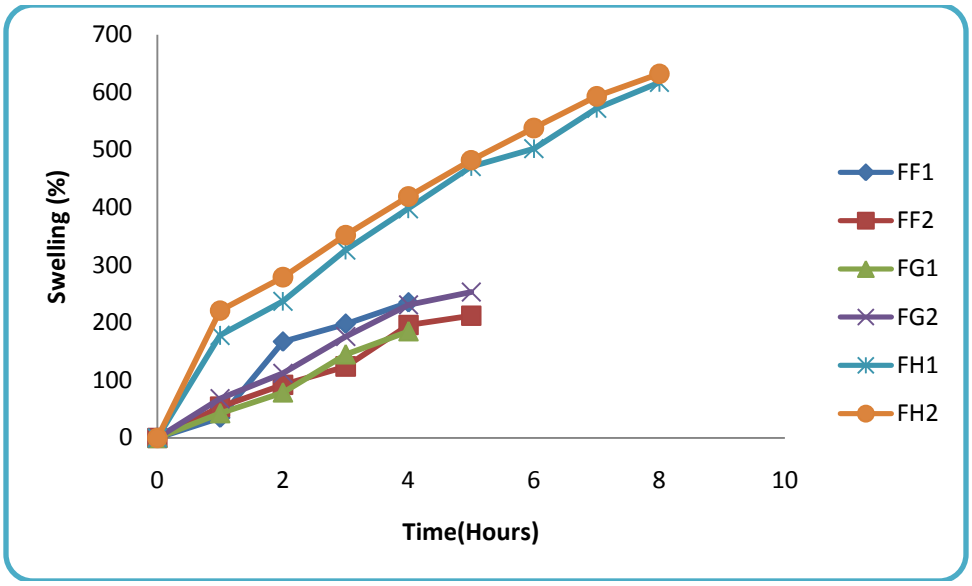

Figure 101A: Swelling index profile for 5-FU formulations FF1-FH2 in SVF pH 4.2

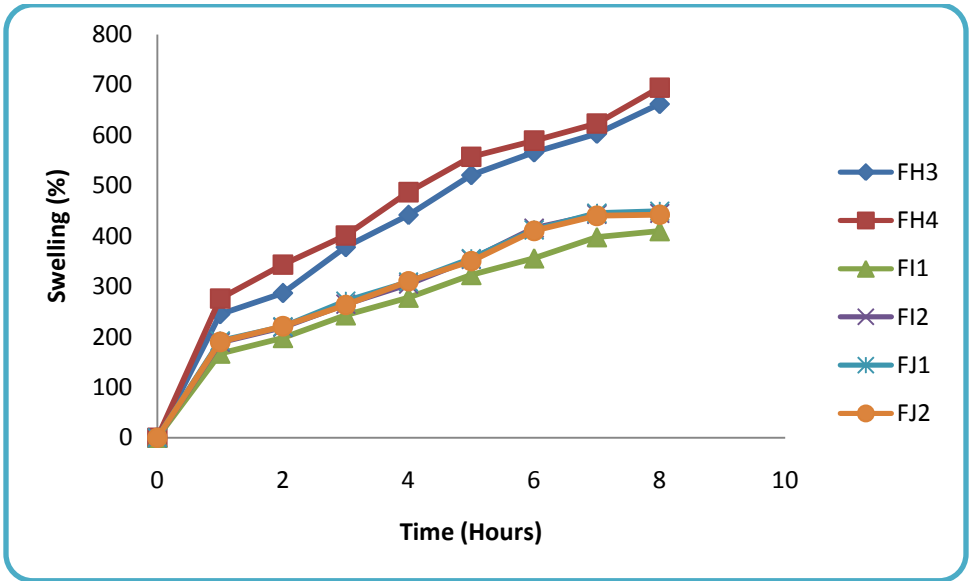

Figure 101B: Swelling index profile for 5-FU formulations FH3-FJ2 in SVF pH 4.2

Table 46: Swelling index data of 5-FU formulations FF1-FJ2 in phosphate buffer pH 7.4

Formulation Code	Swelling index Mean ± S.D*							
	Time in Hours							
	1 hour	2 hour	3 hour	4 hour	5 hour	6 hour	7 hour	8 hour
FF1	93 ±0.47	178 ±0.28	279 ±0.76	384 ±0.22	495 ±0.18	632 ±0.58	698 ±0.52	----
FF2	128 ±0.63	203 ±0.38	298 ±0.77	402 ±0.29	524 ±0.99	674 ±0.55	752 ±0.83	----
FG1	45 ±0.32	95 ±0.83	146 ±0.22	197 ±0.11	263 ±0.28	302 ±0.39	---	----
FG2	97 ±0.38	203 ±0.12	253 ±0.27	298 ±0.88	376 ±0.28	397 ±0.37	---	---
FH1	208 ±0.82	278 ±0.37	320 ±0.29	389 ±0.77	470 ±0.28	511 ±0.27	580 ±0.28	622 ±0.25
FH2	217 ±0.99	265 ±0.72	332 ±0.58	410 ±0.48	465 ±0.39	520 ±0.28	585 ±0.73	635 ±0.37
FH3	235 ±0.73	290 ±0.55	372 ±0.37	440 ±0.28	502 ±0.66	538 ±0.58	606 ±0.67	663 ±0.29
FH4	252 ±0.38	325 ±0.58	401 ±0.73	458 ±0.28	544 ±0.22	602 ±0.38	630 ±0.27	687 ±0.21
FI1	113 ±0.27	128 ±0.92	165 ±0.32	244 ±0.62	278 ±0.32	326 ±0.28	349 ±0.82	392 ±0.77
FI2	147 ±0.78	221 ±0.37	256 ±0.83	295 ±0.28	346 ±0.61	435 ±0.32	452 ±0.36	492 ±0.28
FJ1	145 ±0.85	220 ±0.36	251 ±0.28	293 ±0.37	342 ±0.62	432 ±0.88	451 ±0.72	490 ±0.38
FJ2	144 ±0.92	220 ±0.88	253 ±0.39	294 ±0.36	345 ±0.68	435 ±0.29	451 ±0.87	492 ±0.84

***Standard deviation, n = 3**

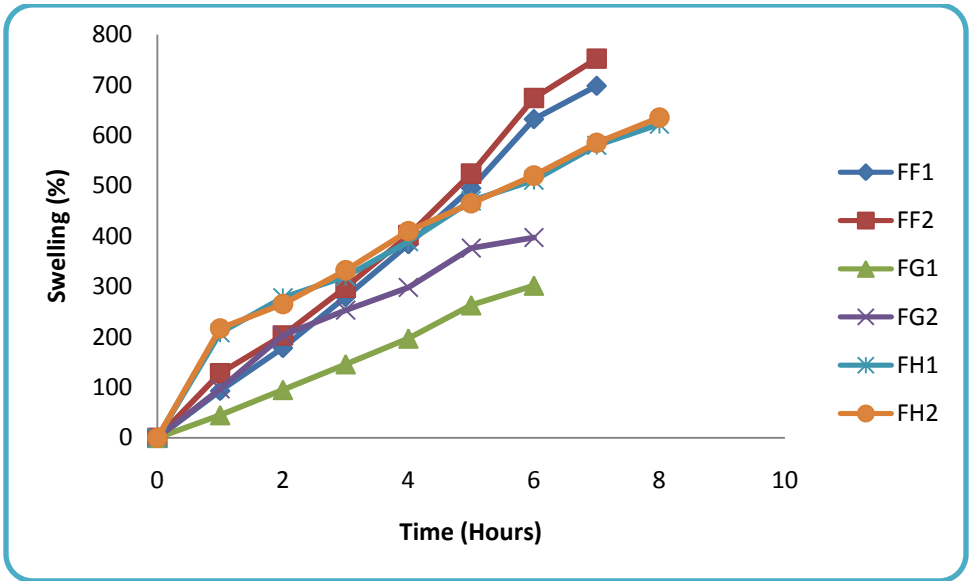

Figure 102A: Swelling index profile for 5-FU formulations FF1-FH2 in phosphate buffer pH 7.4

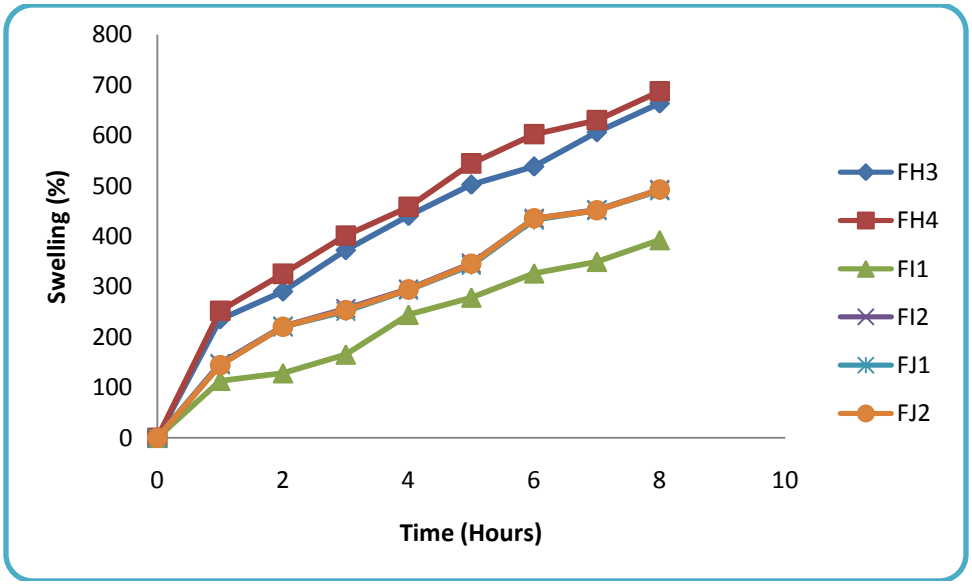

Figure 102B: Swelling index profile for 5-FU formulations FH3-FJ2 in phosphate buffer pH 7.4

6.4.6 *In vitro* dissolution studies

The dissolution data of the individual formulations in phosphate buffer pH 6.8, simulated vaginal fluid pH 4.2 and phosphate buffer pH 7.4 are shown in the table 47, 48 and 49 respectively and graphical representation are given in figures 103A, 103B, 104A,104B and 105A, 105B respectively.

In phosphate buffer pH 6.8, alginate matrices (FF1 formulation) could be attributed to the formation of a less effective diffusion barrier due to fewer polymer particles available for the formation of a continuous and resistant gel barrier. Further increase in polymer concentration (FF2 formulation) reduced the release-retarding effect of the polymer. The most common reason used to explain the effect of polymer content on drug release was that an increase in polymer content resulted in increased viscosity of the gel matrix, causing a reduction in the effective diffusion coefficient of the drug [252]. The alginate matrix tablets showed that the integrity of the matrices was adversely affected during the dissolution study. Varying patterns of deformation, depicted by the presence of surface cracks, grooves and lamination were observed. The extent of deformation was greater at higher alginate concentrations. As alginate content increased, the extent of matrix swelling increased due to greater liquid imbibitions. The latter caused pressure build-up within the matrix which could be released by matrix deformation. In the acidic medium, the conversion of sodium alginate to insoluble alginic acid which could swell without generating surface stickiness could further contribute to the inability of the matrices to maintain their integrity. These effects might have compromised the gel barrier developing around the matrix and exposed greater surface area to the dissolution medium. Hence, the drug released is faster than phosphate buffer pH 6.8 and pH 7.4.

In phosphate buffer pH 7.4, there was rapid formation of gel layer around the tablet, causing a reduction in the effective diffusion of the drug. But the drug release is gradual, Inspite of rapid gel layer around the matrix. This may be due surface cracks and grooves in gel matrix or also may be the higher solubility of 5-fluorouracil which is able to penetrate the gel layer faster [253]. In the case of FG1 formulation, in simulated vaginal pH 4.2, there is an initial burst effect seen visually in the early stage of the dissolution run. This phase may be due to the less hydration or less gel formation of chitosan in acidic pH or may be low concentration of sodium alginate that is not able to produce the desired gel matrix or due to higher concentration of microcrystalline cellulose, which shows disintegration action at higher concentration by rapidly invading dissolution medium using capillarity through available pores in the matrix. After this initial phase, there was swelling of matrix and formation of gel causing clogging of pores, thus hindering the entrance of dissolution medium, which then occured by slow diffusion through the gel layer [254]. In phosphate buffer pH 6.8 and 7.4, there was also initial burst effect but to lesser extent than simulated vaginal pH 4.2. This effect may be lesser due to easy hydration and gelation of sodium alginate, leading to early clogging of available pores in the matrix and, therefore, much slower tablet disintegration and drug dissolution. Although the number of available positive chitosan molecules decreases in buffer, there is an increase in available negative alginate molecules. This may change the packing arrangement of the tablet components. The overall effect will result in a different pattern of dissolution compared with that in buffer. With further increase in the concentration of polymers, the initial burst effect is inhibited which may be due to less concentration of microcrystalline cellulose or may be due to higher concentration of

sodium alginate polymer that inhibits the disintegration activity of microcrystalline cellulose. IPEC containing formulation on contact with phosphate buffer pH 6.8 or 7.4 or simulated vaginal fluid pH 4.2 undergo swelling-driven phase transition. IPEC formulation forms swells and form different microdomain gel layer around matrix and sustain the drug release [255]. With further increase in the concentration there is further thicker gel layer around matrix hence further retarded drug release. FI1 formulation containing chitosan and sodium alginate along with IPEC exhibits varied dissolution profiles. In simulated vaginal pH 4.2, there is gradual drug release pattern as the chitosan forms gel in acidic condition and in sodium alginate also forms gel to lesser extent whereas in phosphate buffer pH 6.8 and 7.4 there is initial burst release due to the presence of chitosan that tend to escape from the gel layer. Hence, there is rapid release of drug. However, in FI2 formulation there is gradual drug release as the concentration of polymers increased, as sodium alginate tend to neutralize the chitosan effect and there is very less concentration of microcrystalline cellulose that doesn't favor the disintegration effect of chitosan inspite of higher concentration.

FJ1 and FJ2 formulation contains similar polymer concentration as FI2 formulation but there is an addition of sodium deoxycholate which acts as permeation enhancer. The drug release profile from FJ1 and FJ2 formulation exhibits similar drug release profile as FI2 formulation. Hence the presence of permeation enhancer doesn't have influence on drug release profile which is in agreement with the reported studies [222].

Table 47: *In vitro* dissolution data of 5-FU formulations FF1-FJ2 in phosphate buffer pH 6.8

Formulation Code	Drug Release (%)							
	1 hour	2 hour	3 hour	4 hour	5 hour	6 hour	7 hour	8 hour
	Mean ± S.D*							
FF1	18.36 ±0.48	33.14 ±0.92	53.65 ±1.31	72.42 ±0.24	85.25 ±0.27	97.73 ±0.32	---	---
FF2	13.22 ±0.27	27.76 ±0.88	40.18 ±0.52	57.73 ±0.25	71.48 ±0.16	83.18 ±0.26	91.47 ±0.15	95.27 ±0.25
FG1	35.72 ±0.21	56.87 ±0.18	74.28 ±0.26	82.57 ±1.62	94.27 ±0.22	98.25 ±0.37	----	----
FG2	25.77 ±0.84	41.36 ±0.26	62.54 ±0.22	69.25 ±0.78	80.82 ±1.09	93.62 ±0.58	96.22 ±0.23	----
FH1	17.82 ±0.83	34.72 ±0.87	48.28 ±0.36	65.88 ±0.27	78.28 ±0.65	88.25 ±0.37	96.25 ±1.46	99.22 ±0.36
FH2	15.37 ±0.37	30.51 ±0.27	53.22 ±0.16	62.41 ±0.38	75.22 ±0.92	83.22 ±0.22	92.17 ±1.21	96.35 ±0.37
FH3	11.21 ±0.83	24.37 ±0.25	34.36 ±0.87	45.26 ±1.20	56.62 ±0.37	72.66 ±0.72	86.27 ±0.24	93.22 ±0.18
FH4	9.32 ±0.33	15.21 ±0.21	26.88 ±0.37	38.28 ±0.82	46.18 ±0.21	62.58 ±0.29	71.74 ±0.92	74.27 ±1.65
FI1	45.22 ±0.11	52.18 ±0.82	58.27 ±0.27	69.22 ±0.18	84.21 ±0.48	93.26 ±0.25	96.27 ±0.71	98.35 ±0.26
FI2	14.25 ±0.98	23.37 ±0.27	37.72 ±0.81	52.16 ±0.77	67.82 ±0.29	78.82 ±0.46	90.25 ±0.57	97.25 ±0.68
FJ1	12.87 ±0.37	20.52 ±0.25	34.72 ±0.28	51.86 ±0.59	66.39 ±0.92	77.29 ±0.28	90.72 ±0.74	95.38 ±0.15
FJ2	12.41 ±0.15	22.47 ±0.38	35.83 ±0.52	55.26 ±0.82	64.82 ±0.28	76.27 ±1.02	91.48 ±0.37	96.88 ±0.11

***Standard deviation, n = 3**

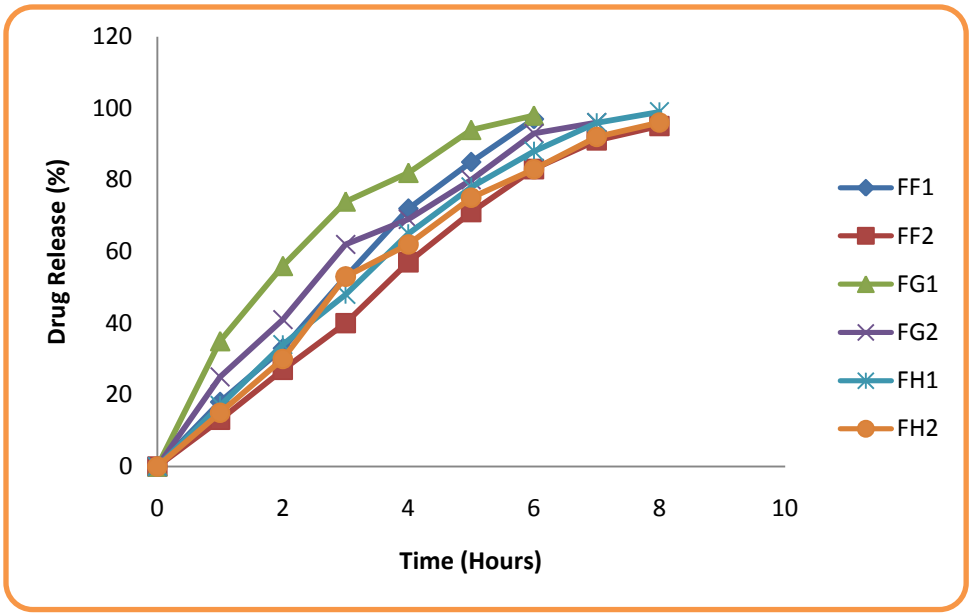

Figure 103A: 5-FU release profile of formulations FF1-FH2 in phosphate buffer pH 6.8

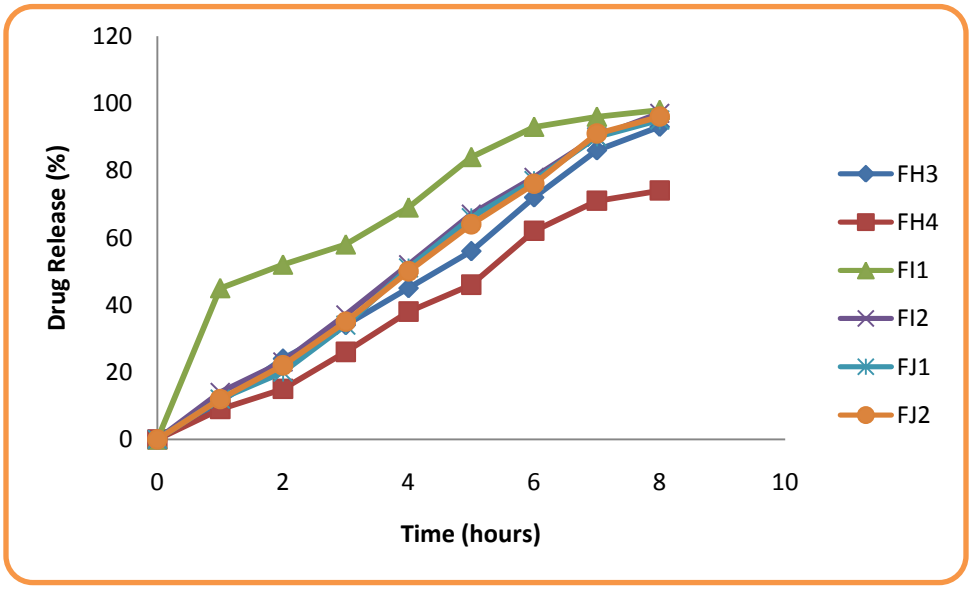

Figure 103B: 5-FU release profile of formulations FH3-FJ2 in phosphate buffer pH 6.8

Table 48: *In vitro* dissolution data of 5-FU formulations FF1-FJ2 in SVF pH 4.2

Formulation Code	Drug Release (%)							
	1 hour	2 hour	3 hour	4 hour	5 hour	6 hour	7 hour	8 hour
	Mean ± S.D*							
FF1	27.37 ±0.83	59.11 ±0.71	82.73 ±0.28	93.72 ±0.22	99.27 ±0.26	----	---	-----
FF2	21.47 ±0.26	43.82 ±0.18	64.19 ±0.28	84.28 ±0.13	98.26 ±0.28	----	----	-----
FG1	45.28 ±0.28	55.21 ±1.23	78.19 ±0.92	88.29 ±0.19	97.12 ±0.29	----	----	----
FG2	19.28 ±0.11	38.81 ±0.82	58.22 ±0.61	81.26 ±0.25	93.28 ±0.55	----	----	----
FH1	22.57 ±0.52	37.28 ±0.28	55.21 ±0.91	68.28 ±1.01	76.22 ±0.82	87.25 ±0.27	94.27 ±0.18	98.25 ±0.28
FH2	19.56 ±0.64	32.58 ±0.26	50.24 ±0.83	59.38 ±0.22	70.37 ±0.34	78.26 ±0.92	90.25 ±0.19	96.56 ±0.28
FH3	15.25 ±0.72	24.82 ±0.28	34.26 ±0.18	47.28 ±0.58	56.26 ±0.29	70.35 ±0.22	85.22 ±0.81	95.26 ±0.65
FH4	9.64 ±0.36	14.52 ±1.21	24.67 ±0.73	36.91 ±0.25	48.88 ±0.85	62.65 ±0.28	70.71 ±0.26	81.62 ±0.67
FI1	12.46 ±0.57	22.58 ±0.92	37.72 ±0.28	53.29 ±0.72	64.22 ±0.26	75.28 ±0.15	81.71 ±0.21	90.26 ±0.26
FI2	12.28 ±0.67	20.57 ±0.23	35.82 ±0.82	48.68 ±0.67	60.28 ±0.28	75.81 ±0.68	89.22 ±0.67	97.25 ±0.22
FJ1	12.33 ±0.68	19.92 ±0.92	34.58 ±0.57	48.27 ±0.73	60.28 ±0.81	75.25 ±0.31	88.26 ±0.27	96.26 ±0.78
FJ2	12.25 ±0.58	20.32 ±0.22	35.28 ±0.96	48.29 ±0.25	59.17 ±0.58	74.38 ±0.28	89.37 ±0.37	96.23 ±0.28

***Standard deviation, n = 3**

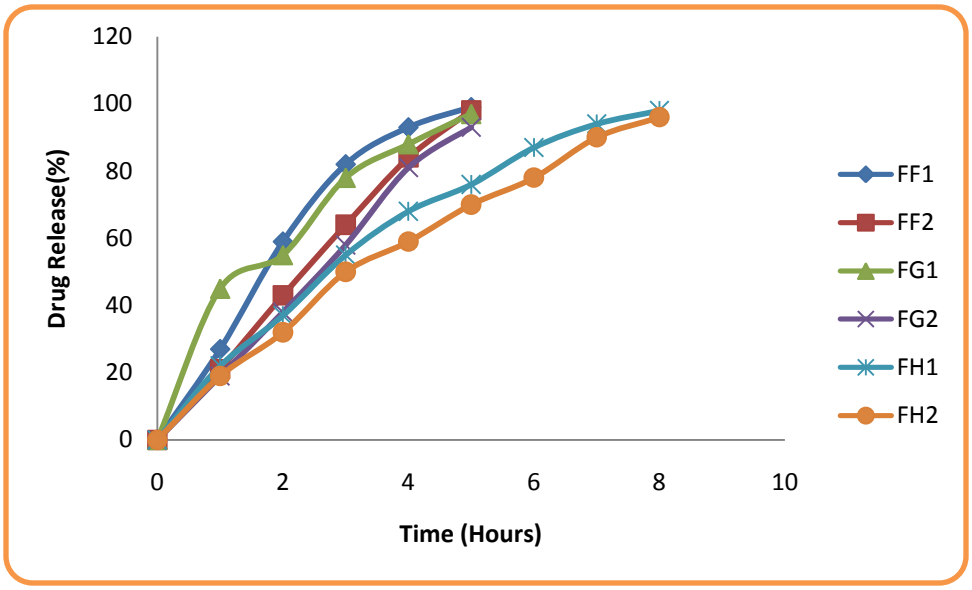

Figure 104A: 5-FU release profile of formulations FF1-FH2 in SVF pH 4.2

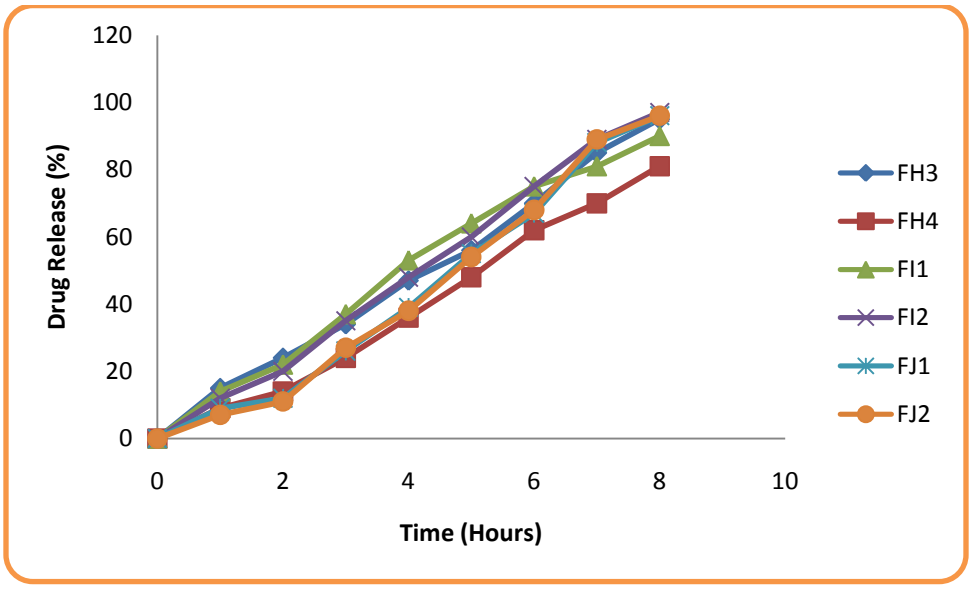

Figure 104B: 5-FU release profile of formulations FH3-FJ2 in SVF pH 4.2

Table 49: *In vitro* dissolution data of 5-FU formulations FF1-FJ2 in phosphate buffer pH 7.4

Formulation Code	Drug Release (%)							
	1 hour	2 hour	3 hour	4 hour	5 hour	6 hour	7 hour	8 hour
	Mean ± S.D*							
FF1	26.38 ±0.92	45.29 ±0.72	61.47 ±0.41	84.59 ±0.29	95.28 ±0.28	----	----	----
FF2	19.75 ±0.83	31.58 ±0.92	54.39 ±0.22	79.21 ±0.15	85.10 ±0.28	96.28 ±0.21	----	----
FG1	35.92 ±0.18	59.21 ±0.85	78.29 ±0.77	90.19 ±0.91	97.17 ±0.26	----	----	-----
FG2	25.11 ±0.18	51.48 ±0.24	73.21 ±0.11	85.29 ±0.15	94.80 ±0.17	----	-----	----
FH1	22.54 ±0.98	35.18 ±0.12	52.58 ±1.05	65.21 ±0.86	76.19 ±0.64	86.27 ±0.18	95.71 ±0.81	98.57 ±0.64
FH2	20.68 ±0.69	32.96 ±0.19	42.60 ±0.93	54.66 ±1.31	71.68 ±0.81	81.27 ±0.68	92.68 ±0.16	97.85 ±0.63
FH3	17.93 ±0.68	30.68 ±0.19	39.92 ±1.08	48.18 ±0.23	62.56 ±0.83	78.29 ±0.84	87.22 ±0.11	90.53 ±0.15
FH4	8.54 ±0.59	13.61 ±0.17	20.77 ±0.62	33.64 ±0.83	45.19 ±0.86	61.77 ±0.26	74.28 ±0.62	78.31 ±0.55
FI1	15.68 ±0.18	28.13 ±0.72	37.92 ±0.67	48.22 ±0.29	60.38 ±0.39	75.39 ±0.61	85.39 ±0.81	95.71 ±1.44
FI2	14.11 ±0.75	27.95 ±0.92	35.29 ±1.54	49.55 ±0.59	64.31 ±0.82	73.18 ±0.76	88.38 ±0.38	94.22 ±0.68
FJ1	13.55 ±0.75	26.02 ±0.38	33.68 ±0.86	48.26 ±0.72	63.29 ±0.53	72.68 ±0.63	88.39 ±0.22	94.28 ±0.62
FJ2	13.51 ±0.52	27.69 ±0.86	34.21 ±0.69	48.60 ±0.15	63.77 ±0.26	73.96 ±0.61	88.19 ±0.28	95.29 ±0.11

***Standard deviation, n = 3**

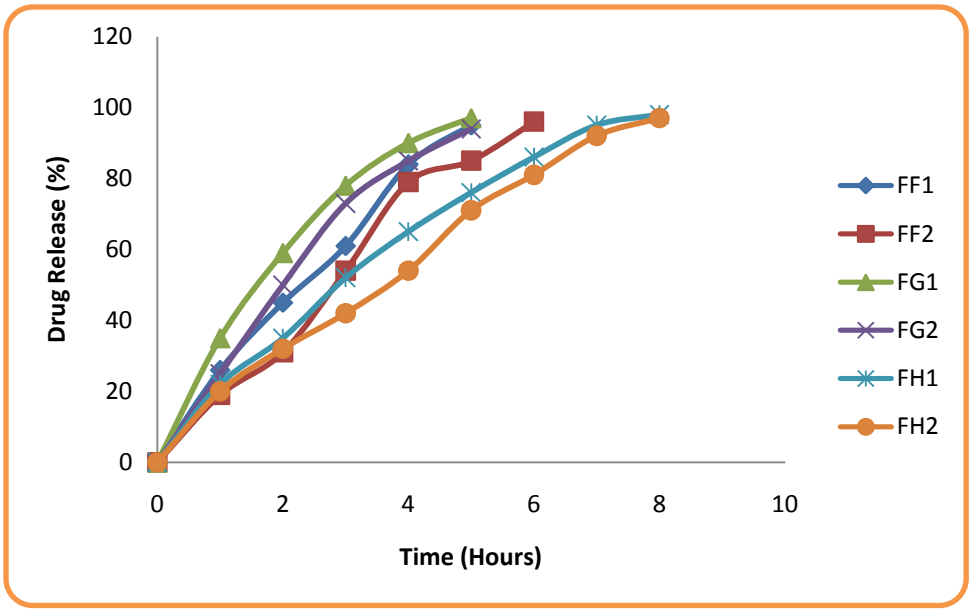

Figure 105A: 5-FUrelease profile of formulations FF1-FH2 in phosphate buffer pH 7.4

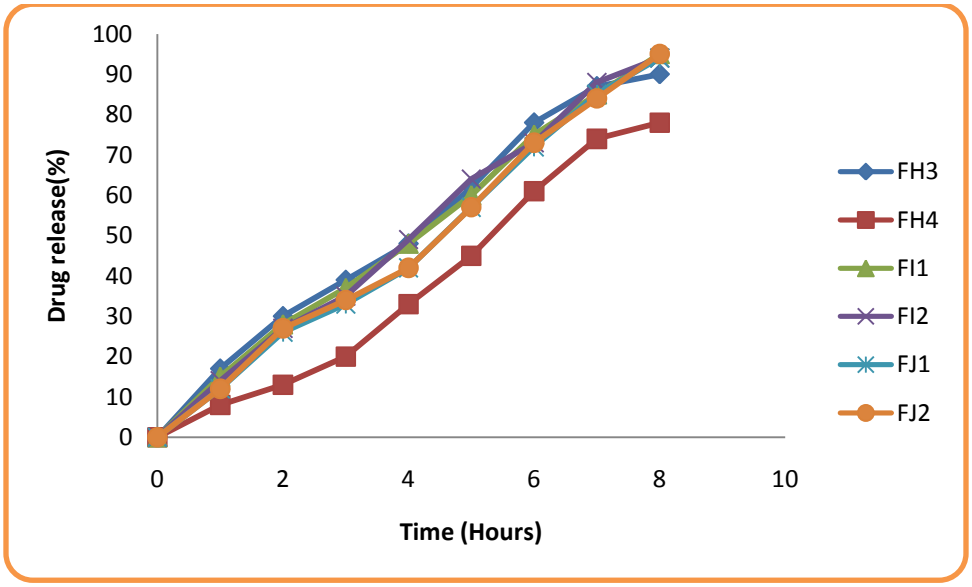

Figure 105B: 5-FUrelease profile of formulations FH3-FJ2 in phosphate buffer pH 7.4

The above results showed that IPEC formulations exhibited pH independent drug release. The presence of chitosan and sodium alginate altered the drug release profile. However, FI2 (FJ1 or FJ2) formulation was considered as optimized formulation based on the *in vitro* drug release studies and it was subjected to similarity factor study.

To confirm the similarity of FI2 formulation dissolution profiles in phosphate buffer pH 6.8, simulated vaginal fluid pH4.2 and phosphate buffer pH 7.4, the similarity factor (f_2) was calculated and summarized in the table 50.

Table 50: Similarity factor (f_2) values calculated for the dissolution profiles of FI2 formulation between different buffer solutions

Comparison	Similarity factor (f_2)
FI2(Buccal pH) vs FI2 (Vaginal pH)	73.14
FI2 (Buccal pH) vs FI2 (Rectal pH)	69.97

Since the f_2 values were higher than 50 (as per USFDA guidelines), these results confirmed that the drug release profiles were almost similar for FI2 formulation for buccal, vaginal and rectal pH.

6.4.7 *In vitro* mucoadhesion studies

Mucodhesive strength for formulations (FH1-FJ2) are summarized in table 51 and represented in figure 106 respectively. Based on the *in vitro* desired drug release profile, formulations FH1-FJ2 were subjected for the mucoadhesive studies. Four formulations containing IPEC exhibited the least mucoadhesive strength. The formed complex lacks the functional groups which are involved in the complex formation; hence they exhibited less mucoadhesive strength. Further increase in the concentration of IPEC, doesn't increase bioadhesive strength. The formed complex lacks the strong binding but finds little binding to the mucosal surfaces via hydrogen bonding interactions [189]. FI2 formulation containing chitosan and sodium alginate exhibits higher mucoadhesive strength than IPEC formulation. The mucoadhesion may be due to various reasons like the presence of free carboxylic groups which provide the ability to form hydrogen bonds is a critical characteristic that is found in sodium alginate polymer and also amine group of chitosan reacts with the mucin. The adhesion of tablets may be also being due to chain penetration of polymers in mucin. Increasing concentration of chitosan and sodium alginate further increases mucoadhesion. The presence of permeation enhancer in FJ1 and FJ2 formulation doesn't produce further mucoadhesion.

Table 51: Mucoadhesive studies data for FH1-FJ2 formulations

Formulation code	Mucoadhesive strength(N/cm^2) Mean±SD*
FH1	0.021±0.008
FH2	0.031±0.01
FH3	0.032±0.01
FH4	0.041±0.007
FI1	0.09±0.01
FI2	0.17±0.018
FJ1	0.17±0.016
FJ2	0.17±0.02

mean±SD, n=3

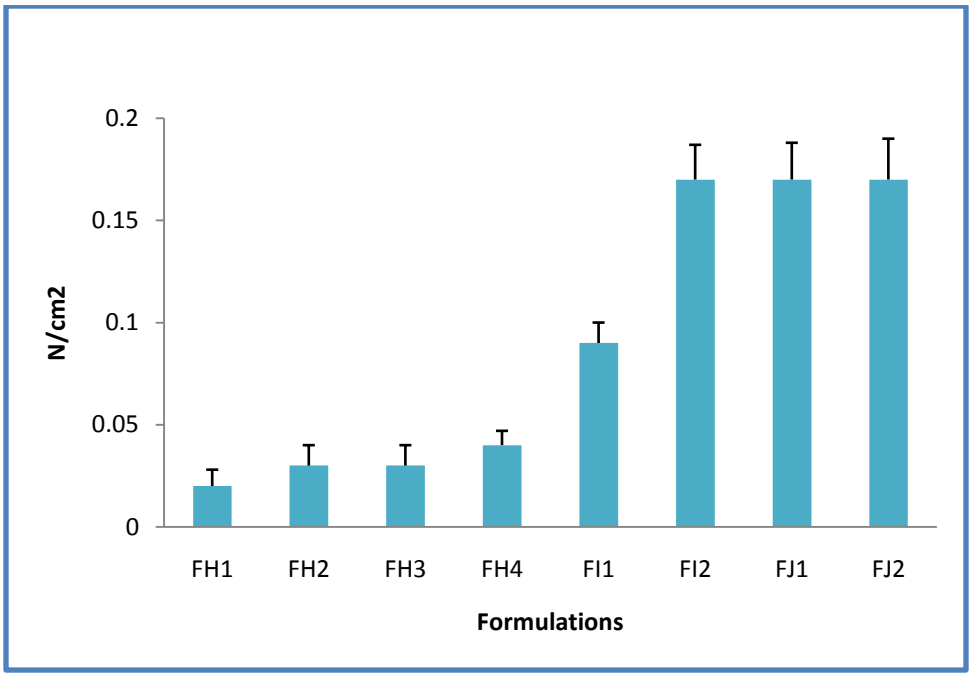

Figure 106: Mucoadhesive strength profile for formulations FH1-FJ2

6.4.8 *In vivo* X-ray studies

The bioadhesion & retention property was studied in albino rabbit. Optimized formulation FI2, developed by using barium sulfate (replacing 20 mg of 5-fluorouracil) was administered to rabbit. The duration of tablet in buccal, vaginal and rectal cavity was monitored by radiograms. It is evident from the pictures that the tablets remained intact and adhered to the buccal, vaginal and rectal mucous membrane for over 8 Hrs. The *in vivo* x-ray radiographic images of optimized matrix tablet in rabbits is given in figure 107.

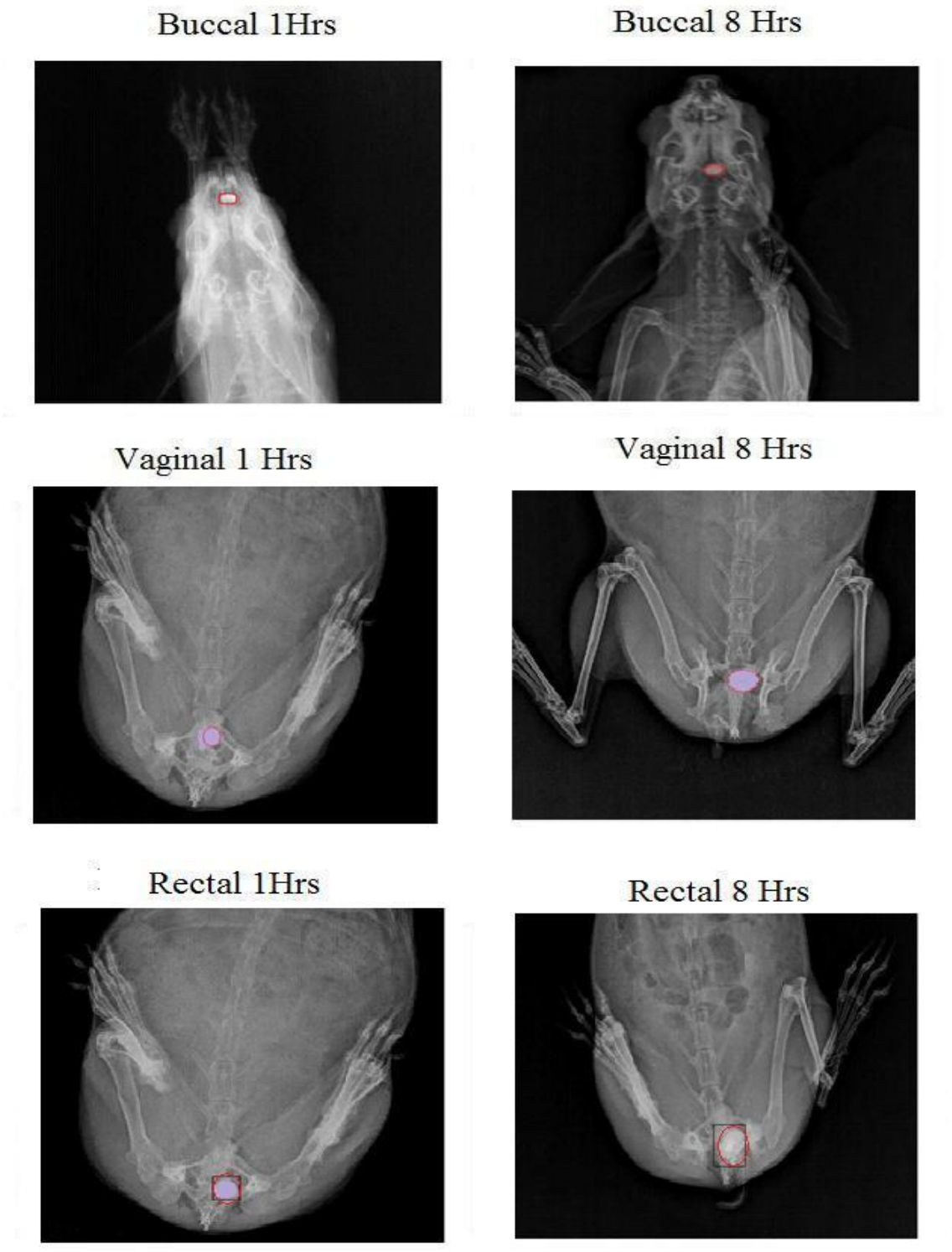

Figure 107. X-ray radiographic images of buccal, vaginal and rectal cavity at 1 and 8 h after ingestion of $BaSO_4$-loaded optimized FI2 matrix tablet in rabbits

6.4.9 Ex vivo permeation studies

5-FU permeation from formulations FJ1 and FJ2 across sheep mucosa over a period of 8 h is shown in Figure 108 and summarized in table 52. The maximum permeation of 5-FU from FJ2 was 99 % at 8 h compared with 60 % from FJ1. Regression of the linear portions of the two plots gave Slopes and intercepts from which the permeation flux (slope divided by mucosal surface area) of FJ1 and FJ2 were calculated to be 8.6 and 5.01 $mg/cm^2/h$, respectively.

In formulation FJ1 addition of SDC 2 % increased the cumulative percentage of drug permeation to 60 %. This may be due to SDC extracted only mucosal lipid from the intercellular spaces. Thus, this enhances the diffusivity of the 5-FU via the par cellular or polar route. Further increase in concentration of SDC (FJ2), i.e., 3 %, increased the drug permeation up to 99 % thus SDC in 3 % extract lipids from the cell membranes, along with the extraction of mucosal lipid from the intercellular spaces by the formation of micelles. This resulted in enhancing passive diffusivity of the 5-FU via transcellular (crossing the cell membranes and entering the cell) and para cellular routes [223]. It was mentioned that SDC can also cause the uncoiling and extension of the protein helices, which leads to opening of the polar pathways for diffusion [224]. All these effects might contribute to enhancing the permeation of the drug.

Table 52: 5-FU permeation data for formulations FJ1 and FJ2

Formulation Code	Drug permeated (%)							
	1 hour	2 hour	3 hour	4 hour	5 hour	6 hour	7 hour	8 hour
	Mean ± S.D*							
FJ1	9.37 ±0.92	15.75 ±0.53	21.62 ±1.82	28.22 ±0.99	36.26 ±1.21	44.82 ±0.89	545.14 ±1.02	60.15 ±0.91
FJ2	16.58 ±1.73	30.43 ±0.84	41.82 ±1.62	56.18 ±0.92	72.17 ±1.72	85.48 ±0.92	95.58 ±1.25	99.11 ±0.72

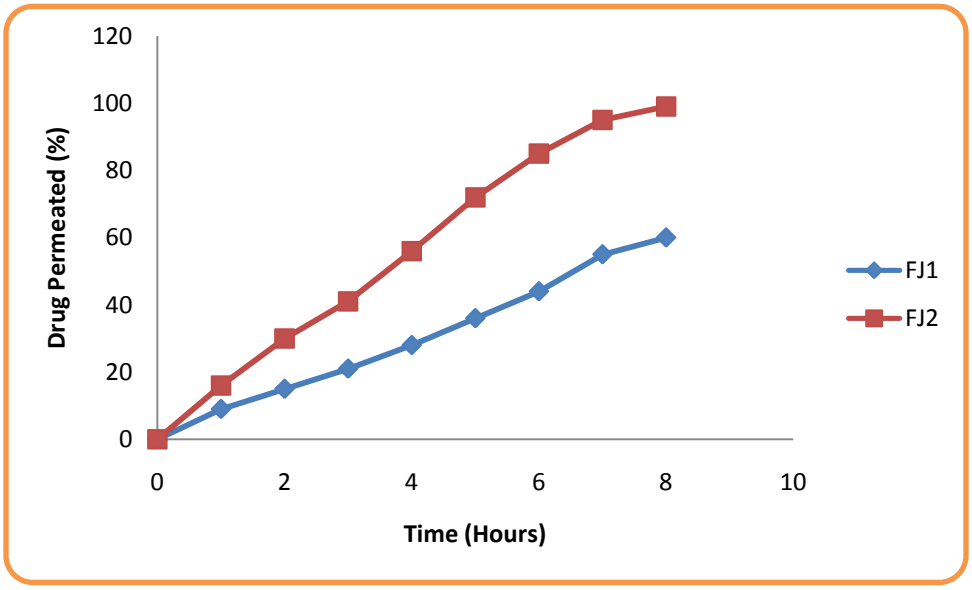

Figure 108: 5-FU permeation profiles of FJ1 and FJ2 formulations

6.4.10 Mathematical model fitting

To ascertain drug release mechanism and release rate, the release data were fitted into release models using PCP Disso V2.01 dissolution software. The parameters like 'n' the time exponent and 'R' the regression co-efficient were determined to know the release mechanisms. The data for the formulations FH1-FI2 are summarized in table 53.

Table 53: Mathematical model fitting data for FH1 to FI2 formulations

Formulation code	Buffer condition	Zero order R	First order R	Matrix R	Peppas		Hixon crowel R
					R	n	
FH1	Buccal pH	0.9906	0.9929	0.9563	0.9972	0.9291	0.9922
	Vaginal pH	0.9700	----	0.9788	0.9959	0.8246	0.9034
	Rectal pH	0.9770	----	0.9753	0.9975	0.7726	0.8987
FH2	Buccal pH	0.9886	0.9912	0.9559	0.9926	0.9685	0.9904
	Vaginal pH	0.9864	0.8815	0.9684	0.9976	0.8246	0.9669
	Rectal pH	0.9923	-----	0.9575	0.9962	0.8133	0.8781
FH3	Buccal pH	0.9964	0.9947	0.9103	0.9990	0.9514	0.9953
	Vaginal pH	0.9980	0.8575	0.9235	0.9952	0.9464	0.9342
	Rectal pH	0.9967	0.8244	0.9445	0.9963	0.8613	0.9348
FH4	Buccal pH	0.9929	0.9917	0.9028	0.9950	0.9147	0.9921
	Vaginal pH	0.9908	0.9354	0.8911	0.9926	0.9771	0.9611
	Rectal pH	0.9826	0.9304	0.8752	0.9884	0.9230	0.9525
FI1	Buccal pH	0.9376	0.9466	0.9857	0.9752	0.8560	0.9437
	Vaginal pH	0.9799	0.9829	0.9740	0.9979	0.7648	0.9974
	Rectal pH	0.9882	0.8254	0.8846	0.9889	0.8460	0.9115
FI2	Buccal pH	0.9982	0.9977	0.9235	0.9965	0.9714	0.9979
	Vaginal pH	0.9871	0.8090	0.8809	0.9983	0.9781	0.9038
	Rectal pH	0.9874	0.7861	0.8830	0.9834	0.9121	0.8919

The FI2 formulation is considered as the best formulation based on the *in vitro* drug release studies and the mucoadhesion studies. The best model fit for FI2 formulation is zero order and the n value in peppas model is between 0.9-1 indicating non-fickian diffusion as the release mechanism.

6.4.11 Stability studies

Stability studies of 5-FU tablet formulation FJ2 was carried out to determine the physical stability of the formulation. The stability studies were carried out at 25±2 °C and 60±5 % RH, 30±2 °C and 65±5 % RH and 40±2 °C and 75±5 % RH for 6 months. The 5-FU content in the formulation was evaluated. The observation of conditions is shown in table 54. There was no significant change in the tablet properties and drug content.

Table 54: Stability studies of formulation FJ2

Sampling interval (Months)	Stability study conditions		
	25±2 °C & 60±5 % RH	30±2 °C & 65±5 % RH	40±2 °C & 75±5 % RH
	% Drug content mean ± S.D*		
0	99.3± 0.78	99.4 ± 0.63	99.5 ± 0.21
3	98.7± 0.51	98.8 ± 0.25	98.8± 0.85
6	98.5± 0.11	98.6 ± 0.51	98.5 ± 0.15

***Standard deviation, n = 3**